MASTER

GEAP-4130

EXPERIMENTAL STUDIES OF TRANSIENT EFFECTS IN FAST REACTOR FUELS

Series I — UO_2 Irradiations

By
J. H. Field

November 15, 1962

Atomic Power Equipment Department
General Electric Company
San Jose, California

UNITED STATES ATOMIC ENERGY COMMISSION • DIVISION OF TECHNICAL INFORMATION

LEGAL NOTICE

This report was prepared as an account of Government sponsored work. Neither the United States, nor the Commission, nor any person acting on behalf of the Commission:

A. Makes any warranty or representation, expressed or implied, with respect to the accuracy, completeness, or usefulness of the information contained in this report, or that the use of any information, apparatus, method, or process disclosed in this report may not infringe privately owned rights; or

B. Assumes any liabilities with respect to the use of, or for damages resulting from the use of any information, apparatus, method, or process disclosed in this report.

As used in the above, "person acting on behalf of the Commission" includes any employee or contractor of the Commission, or employee of such contractor, to the extent that such employee or contractor of the Commission, or employee of such contractor prepares, disseminates, or provides access to, any information pursuant to his employment or contract with the Commission, or his employment with such contractor.

This report has been reproduced directly from the best available copy.

Printed in USA. Price $2.00. Available from the Office of Technical Services, Department of Commerce, Washington 25, D. C.

USAEC Division of Technical Information Extension, Oak Ridge, Tennessee

DISCLAIMER

This report was prepared as an account of work sponsored by an agency of the United States Government. Neither the United States Government nor any agency Thereof, nor any of their employees, makes any warranty, express or implied, or assumes any legal liability or responsibility for the accuracy, completeness, or usefulness of any information, apparatus, product, or process disclosed, or represents that its use would not infringe privately owned rights. Reference herein to any specific commercial product, process, or service by trade name, trademark, manufacturer, or otherwise does not necessarily constitute or imply its endorsement, recommendation, or favoring by the United States Government or any agency thereof. The views and opinions of authors expressed herein do not necessarily state or reflect those of the United States Government or any agency thereof.

DISCLAIMER

Portions of this document may be illegible in electronic image products. Images are produced from the best available original document.

GEAP-4130

METALS, CERAMICS, AND MATERIALS

Fast Ceramic Reactor Development Program

EXPERIMENTAL STUDIES OF TRANSIENT EFFECTS IN FAST REACTOR FUELS

SERIES I

UO_2 IRRADIATIONS

by

J. H. Field

U. S. ATOMIC ENERGY COMMISSION
Contract AT(04-3)-189
Project Agreement 10

ATOMIC POWER EQUIPMENT DEPARTMENT

GENERAL ELECTRIC

SAN JOSE, CALIFORNIA

TABLE OF CONTENTS

	Page
Abstract	1-1
Summary of Conclusions	2-1
Introduction	3-1
Fuel Test Specimen	4-1
Test Program	5-1
Examination of Fuel Following Transient Tests	6-1
Discussion of Results	7-1
Recommendations	8-1
Acknowledgments	9-1
TREAT Capsule Design	A-1
Fuel Fabrication Procedure	B-1
Experimental Techniques for Testing at TREAT	C-1
Irradiation History	C-1
Reactor Power	C-1
Sample Fuel Temperatures - Basis for Estimates	D-1
Integrated Power versus Time	D-2
Comparison and Discussion of Results, TREAT Power versus Specimen Power	D-2
Computer Calculations using Tiger V	D-2
Post-Irradiation Examination Techniques	E-1

LIST OF ILLUSTRATIONS

Number	Title	Page
1	Series I Fuel Test Specimen (with and without internal thermocouples)	4-2
2	TREAT Fuel Sample 1A, Pre- and Post-Irradiation Profile Measurements	6-3
3	TREAT Fuel Sample 1B, Pre- and Post-Irradiation Profile Measurements	6-4
4	TREAT Fuel Sample 1C, Pre- and Post-Irradiation Profile Measurements	6-5
5	TREAT Fuel Sample 1D, Pre- and Post-Irradiation Profile Measurements	6-6
6	TREAT Fuel Sample 1E, Pre- and Post-Irradiation Profile Measurements	6-7
7	Sample 1B, Fuel and Cladding Interior	6-8
8	Post-Irradiation Sectioning of Sample 1D	6-10
9	Post-Irradiation Sectioning of Sample 1E	6-12
10	APED-TREAT Fuel Pin Number 1A	6-13
11	APED-TREAT Fuel Pin Number 1B	6-14
12	APED-TREAT Fuel Pin Number 1C	6-15
13	Sample 1C, Fusion of Pellet Interfaces	6-16
14	Upper Section APED-TREAT Sample 1D	6-18
15	Central Section APED-TREAT Sample 1D	6-19
16	Photomicrographs of Fuel Clad Interface, Sample 1D	6-20
17	Sample 1E Polished Cross Section	6-21
18	Series 1 TREAT Capsule	A-2
19	TREAT Transient Number 384 - APED Sample 1A	C-3
20	TREAT Transient Number 385 - APED Sample 1A	C-4
21	TREAT Transient Number 386 - APED Sample 1A	C-5
22	TREAT Transient Number 387 - APED Sample 1A	C-6
23	TREAT Transient Number 404 - APED Sample 1B	C-7
24	TREAT Transient Number 423 - APED Sample 1C	C-8
25	TREAT Transient Number 438 - APED Sample 1D	C-9
26	TREAT Transient Number 447 - APED Sample 1E	C-10
27	TREAT Transient Number 448 - APED Sample 1E	C-11
28	Sample Power versus Reactor Power APED-TREAT, Series 1	D-3

LIST OF ILLUSTRATIONS (Continued)

Number	Title	Page
29	Capsule 1A Internal Components of Irradiation Assembly	E-2
30	Pre- and Post-Irradiation Gamma Scans of Sample 1D	E-4
31	Capsule 1B, Sectioning Diagram and Sample Locations	E-5

LIST OF TABLES

Number	Title	Page
IV-1	Series I Fuel - As Fabricated Dimensions, etc.	4-4
V-1	Estimated Fuel Temperatures in Series I Tests	5-2
VI-1	Summary of Post-Irradiation Examination of Series I Fuel Samples	6-8
A-1	Summary of Series I Test Apparatus Characteristics	A-4
C-1	TREAT Reactor Parameters for Series I Transients	C-12
C-2	Series I Sample Powers and Estimated Fuel Temperatures	C-13

SECTION I

ABSTRACT

An experimental program to evaluate the performance of FCR and EFCR fuel during transient operation is outlined and the initial series of tests described in some detail. Test results from five experiments in the TREAT reactor, using 1 inch OD SS clad, UO_2 fuel specimens, are compared with regard to fuel temperatures, mechanical integrity, and post-irradiation appearance. Incipient fuel pin failure limits for transients are identified with maximum fuel temperatures in the range of 7000 F. Multiple transient damage to the cladding is likely for transients above the melting point of the fuel.

SECTION II

SUMMARY OF CONCLUSIONS

The mechanical integrity of unirradiated stainless steel clad UO_2 fuel appears to be maintained during single power transients producing maximum fuel temperatures as high as 7000 F. This performance was anticipated in a previous analytical study. [1] For higher maximum fuel temperatures the vapor pressure of UO_2 may exceed the short-time burst pressure of the clad at the ~1600 F mean wall temperature estimated for such transients in a typical sodium-cooled fast reactor and, consequently, rupture of the clad is anticipated.

Over-all thermal expansion of the fuel in extreme single transients, has been found to be a function of internal spaces present in the system prior to the transient pulse. A proposed method of segmenting fuel internally was found effective in preventing clad deformation in single transients up to and slightly beyond, the fuel melting point.

Repeated transients appear likely to cause inelastic clad deformation at a lower temperature than that for a single transient. This is believed due to some ratcheting mechanism in the fuel. In such circumstances, it appears that thermal expansion of the oxide, rather than internal pressure is the prime cause of clad damage. It is probable that design modifications such as stronger or thicker clad would improve the failure limit for repeated transients and that, in the case of EFCR operation, procedures for fuel rotation could be drawn up, thus limiting the number of severe temperature excursions on any one fuel pin. It appears that the provision of radial expansion space within a fuel pin is of questionable value in view of fuel redistribution and central void formation with even a very limited irradiation history. [2]

SECTION III

INTRODUCTION

Interest in fast ceramic reactors stems from their potential to achieve very low fuel costs through long irradiation of ceramic fuel operating at high specific power. The adequate establishment of safety characteristics for this class of reactors is one of the necessary steps in its development and, therefore, there is considerable interest in the performance of the fuel under severe power excursions. In the limiting case, such excursions may cause fuel vaporization and distortion and bursting of the fuel cladding. Some analytical studies of less extreme transients and possible influences on clad integrity for this class of fuel have been described in a preceding report - GEAP-4058. This report describes the result of the first series of experiments following these studies.

A program of fuel capsule irradiations in the TREAT facility at NRTS has been initiated to provide experimental data. This program of experiments is specifically oriented to include fuels of a design similar to those proposed for the large Fast Ceramic Reactor [3] and the Experimental Fast Ceramic Reactor. [4] The areas of major concern in establishing these fuel designs include: (a) the possibility of densification and/or redistribution of the fuel following transient melting; (b) high transient heat fluxes producing thermal stresses leading to deformation or failure of the cladding; [1] (c) clad deformation due to internal pressure from thermal expansion or vapor pressure of the fuel; (d) the desirability in EFCR design of reducing the reactivity effect of gross fuel expansion in order to better evaluate the Doppler effect. [4, 5]

Since determination of transient behavior is the primary objective in these tests, it was desirable to subject the fuel samples to transient of gradually increasing severity up to the limiting conditions for either the fuel or for the TREAT test facility. The TREAT facility is an air-cooled, thermal, heterogeneous system designed to evaluate reactor fuels under conditions simulating various types of nuclear excursions. This reactor was specifically designed to provide quantitative data on the mechanism of melting of fast reactor fuel elements by nuclear heating analogous to a power excursion in a fast reactor core. [6, 7] It is recognized that the comparatively long neutron lifetime of TREAT prohibits an exact simulation of a fast reactor excursion, however provided that power transients are

short (~50 milliseconds) relative to the thermal time constant of the fuel (~16 seconds for 1 inch fuel), most aspects of the experiment are representative.

The tests described herein were performed during the first six months of 1962 and constitute five of the six irradiations originally proposed for Series I. [8] This first series of tests was performed on low-enrichment, UO_2 fueled, large diameter (1.0 inch) rods, and gave an indication of the transient thermal mechanical capability of sodium-cooled SS clad oxide fuels. It was presumed that UO_2 would exhibit generally similar characteristics to the mixed PuO_2-UO_2 oxides of long term interest for FCR's. Furthermore, the low enrichment permitted testing large diameter pins without incurring a severe flux depression. On the basis of findings and conclusions reached from this series of test further transient testing of mixed oxide fuels in both unirradiated (Series II) and irradiated (Series III) conditions is planned. [9]

SECTION IV

FUEL TEST SPECIMEN

4.0 Design

The fuel specimens for Series I testing were based on a particular design concept for EFCR fuel, they should not, however, be considered prototypical. Selection of the fuel specimen dimensions and materials was based upon the design status report for EFCR as of October 31, 1961. [10]

The fuel pin specimens tested in this first series of TREAT tests were composed of UO_2 fuel pellets (~4 per cent enriched) contained in a 1.0 inch OD tube 0.032 inch wall thickness, of type 304 (annealed) stainless steel (see Figure 1). The total length of the fuel specimens (including end plugs) was 15-3/8 inches. This length was partitioned into four compartments by use of refractory metal disks resting on nickel rings which were spot welded to the cladding tube. Each compartment contained sufficient void to allow for the calculated thermal expansion of the fuel up to its melting point (a 14 mil diametral gap and approximately 70 mils axially). In order to compensate for high thermal stresses, due to radial temperature profile, the partitions had four radial slots to minimize tangential stresses. They were also dished slightly to provide easier means for thermal expansion. Nickel was selected as the support ring material due to its high strength, properties at elevated temperatures, and an expansion coefficient calculated to result in minimum stress at the spot welds. In the various tests of Series I provisions have been made to assess: -

- Maximum fuel temperature
- Total heat generation
- Internal pressure generation
- Axial and radial expansion of the fuel

Further details of the design basis for the fuel are given in reference (1).

4.1 Instrumentation

As shown in Figure 1, the first test specimen (No. 1A) contained a thermocouple for measurement of fuel temperature. The purpose of this thermocouple was to allow an initial correlation of reactor

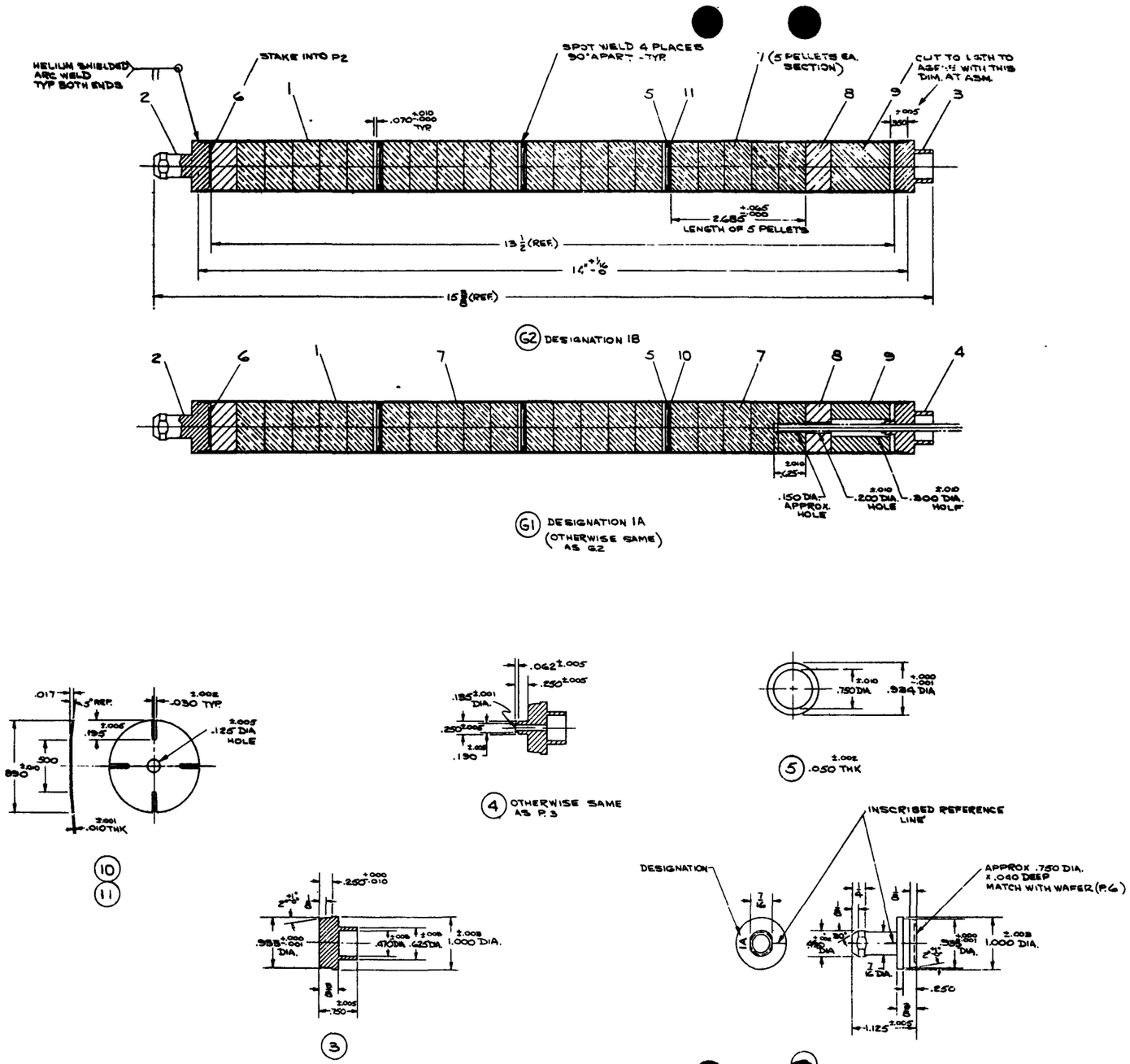

NO. 762D603	TITLE ASM FUEL ELEMENT (WITH & WITHOUT INTERNAL THERMOCOUPLE) FIRST MADE FOR SERIES 1 TREAT TESTS				
		G2	G1	PART NO.	NAME	DRAWING NO., DESCRIPTION, MATERIAL, WEIGHT
		1	1	1	TUBE	.936±.005 ID (.032 WALL) 304 STN. STL.
		1	1	2	BOTTOM END PLUG	304 STN. STL.
			1	3	TOP END PLUG	304 STN. STL.
		1		4	TOP END PLUG	304 STN. STL.
		3	3	5	PARTITION RING	"A" NICKEL (99.4% Ni + Co)
		1	1	6	WAFER	.750 DIA. x .040 THK (APPROX) COBALT
		20	20	7	FUEL PELLET	.922±.002 DIA. 3.9% ENRICHED UO_2
						O/U RATIO ≤ 2.03
		2	2	8	INSULATOR	.922±.002 x 1/2 LG. THORIA (ThO_2)
		1	1	9	FILLER PLUG	.300±.010 DIA. x 1 3/32 APPROX. 304 STN. STL.
			3	10	PARTITION DISK	TANTALUM
		3		11	PARTITION DISK	TUNGSTEN

FIGURE 1

(W/AND W/O INTERNAL THERMOCOUPLE)

power with fuel temperature in a series of small preliminary transients. This tantalum-sheathed, platinum/platinum - 10 per cent rhodium couple was brazed through the upper end plug and operated up to a maximum temperature of 3200 F. Subsequent elements in Series I, being of similar fuel enrichment and using identical test capsules, did not employ an internal thermocouple.

In the last three samples tested (1C, 1D and 1E) the steel filler plug at the upper end was replaced by an extensometer to measure the axial expansion of the top fuel section. This device consisted of two concentric pieces of stainless steel tubing which overlaped with an ~0.003 inch interference fit, and required a force of 2 to 4 pounds to cause a decrease in length. In addition, the last two specimens (1D and 1E) were equipped with pressure transducers [9] to sense the gas pressures generated within the pin. These transducers were a variable reluctance type by International Resistance Company and were connected to the fuel space via a hole in the upper end plug.

4.2 Fabrication and Assembly

Fabrication of the 1 inch diameter UO_2 pellets in the stainless steel clad and the subsequent assembly in sodium filled test capsules is outlined in Appendix B-1.

Table IV-1 summarizes the important physical parameters of the five as fabricated Series I fuel specimens.

TABLE IV-1

SERIES I FUEL - AS FABRICATED DIMENSIONS, ETC.

FUEL							RING	DISK		REMARKS
Sample No.	Length, in.	Dia., in.	Weight, grams	Density % of TD	Enrichment %	O/U Ratio	Thickness, in.	Material	Thickness, in.	
1A	10.775	0.921	1209	93.6	3.9	2.003	0.150	Ta	0.010	1/8 inch hole drilled in upper two pellets to accomodate thermocouple.
1B	10.828	0.921	1214	93.6	3.9	2.003	0.050	W	0.010	Slope control used on spot welds.
1C	10.563	0.921	1191	94.2	3.9	2.003	0.050	W	0.010	First pin to contain extensometer.
1D	10.737	0.921	1226	95.3	4.0	2.016	0.050	W	0.005	First pin to be equipped with pressure transducer.
1E	10.714	0.921	1223	95.4	4.0	2.016	0.050	W	0.005	

SECTION V

TEST PROGRAM

The experimental objectives for the Series I TREAT tests of FCR fuel can be summarized in the following terms: -

1. To carry out transient tests of gradually increasing severity, guided approximately by prior analytical work, in order to determine the point beyond which major mechanical damage becomes evident.
2. To evaluate the possible influence of repeated transients in the vicinity of this limiting value to see if any cumulative damage mechanisms evidence themselves.

On the basis of these objectives, sample power and resultant maximum fuel temperatures become the most important pieces of information in the program. Table V-1 indicates the actual transient tests carried out in Series I and the maximum fuel temperatures estimated for each of them.

TABLE V-1

ESTIMATED FUEL TEMPERATURES IN SERIES I TESTS

(For details of method of determination, etc. see Appendix D-1)

Sample and Transient	Peak Fuel Temp. °F	Comment
1A - 1	1,040)	Experiment calibration
- 2	1,820)	leading to 1A-4 planned
- 3	2,520)	1st test.
- 4	4,090)	
1B -	5,000	Test into melting range
1C	5,220	Test well beyond MPt
1D	7,370	Test into vaporization range
1E - 1	4,670)	
- 2	5,570)	
- 3	5,650)	Repeated transients -
- 4	5,710)	all but first taking fuel
- 5	5,820)	well beyond melting point.
- 6	6,010)	
- 7	5,920)	

SECTION VI

EXAMINATION OF FUEL FOLLOWING TRANSIENT TESTS

6.0 General

Post irradiation examination did not reveal the mechanical integrity of the clad breeched in any of the specimens, although in some cases severe distortion was evident. The fuel vaporization point was reached in at least one test. There was, however, a general progression of clad deformation from mild to more severe transients and a strong indication that repeated transients result in increased clad damage possibly even with relatively mild transients. These findings are summarized in Table VI-1, and further details enumerated below:

6.1 Fuel Dimensional Changes

Figures 2 through 6 illustrate the comparison of diametral and profile measurements before and after testing. It can be seen from these figures that no significant deformation was noted until the examination of sample No. 1D. Measurement of this specimen revealed a definite increase in cladding diameter (up to 20 mils at some locations), as well as a 0.050 inch increase in over-all specimen length. Specimen No. 1E was found to have sustained changes in diameter from +0.050 inch to -0.050 inch. The average of post-irradiation length measurements indicated a 0.090 inch axial increase in the cladding for this pin.

6.2 Changes in Fuel Appearance Resulting from Transient

The appearances of the first three fuel specimens following irradiation were very similar. All pellets were fractured but were easily separated and there was no evidence of melting or gross fusion between pellets. The position of the internal rings and disks was unchanged but the gaps left for fuel expansion had been taken up to a varying degree by apparent fuel movement. Figure 7 is an example of the typical appearance of the fuel specimen interior after sectioning. The disks were very brittle and fractured during remote handling.

The interior view of specimen No. 1D was markedly different than previous samples. There was considerable evidence of UO_2 melting and even possible vaporization in the central regions of the fuel.

TABLE VI-1

SUMMARY OF POST-IRRADIATION EXAMINATION OF SERIES I FUEL SAMPLES

Capsule Number	Irradiation History (reactor power)	Estimated Sample Temperatures °F	Sample Burnup MWD/T	Post-Irradiation Examination								Remarks
				Pellet cracking	Fuel movement	Clad deformation	Grain growth	Pellet fusion	Columnar grains	Molten UO_2	Central void	
1A	4 transients 19, 89, 162 and 315 MWs	Peak 4100 Avg. 3700	1.87×10^{-2}	yes	slight	no	no	no	no	no	no	
1B	1 transient 420 MWs	Peak 5000 Avg. 4900	1.35×10^{-2}	yes	yes	no	slight	no	no	no	no	
1C	1 transient 585 MWs	Peak 5200 Avg. 5000	1.64×10^{-2}	yes	yes	no	yes	some	no	no	no	4 per cent axial fuel expansion in uppermost section
1D	1 transient 765 MWs	Peak 7300 Avg. 6600	2.34×10^{-2}	yes	yes	yes	yes	yes	yes	yes	yes	Extensive central void and vapor bubbles
1E	7 transients 575 MWs (typical)	Peak 5700 Avg. 5000 (typical)	9.4×10^{-2}	yes	yes	yes	yes	yes	no	?	yes	Intermittent central void with some vapor bubbles

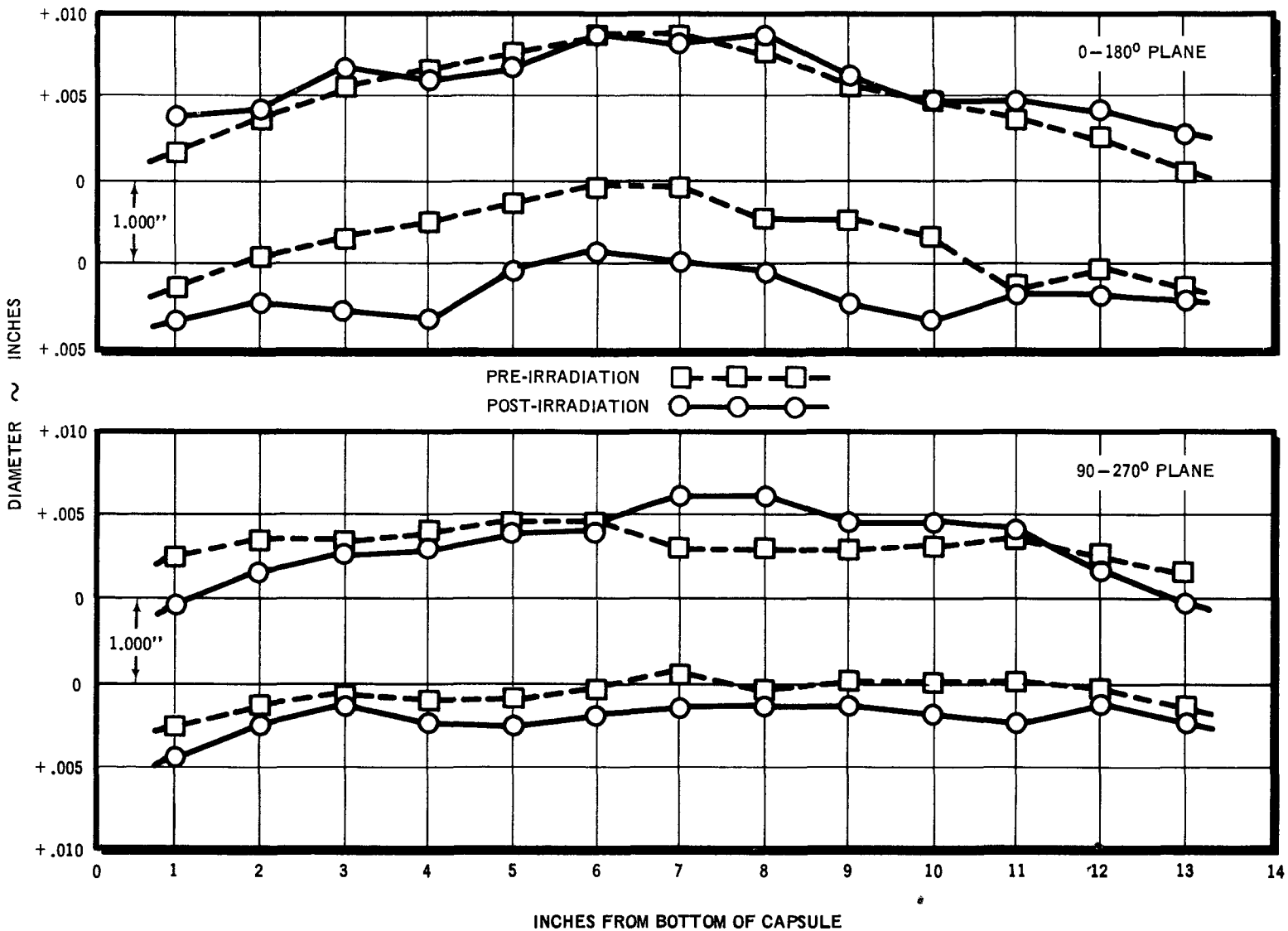

FIGURE 2 TREAT FUEL SAMPLE NO. 1A, PRE AND POST IRRADIATION PROFILE MEASUREMENTS

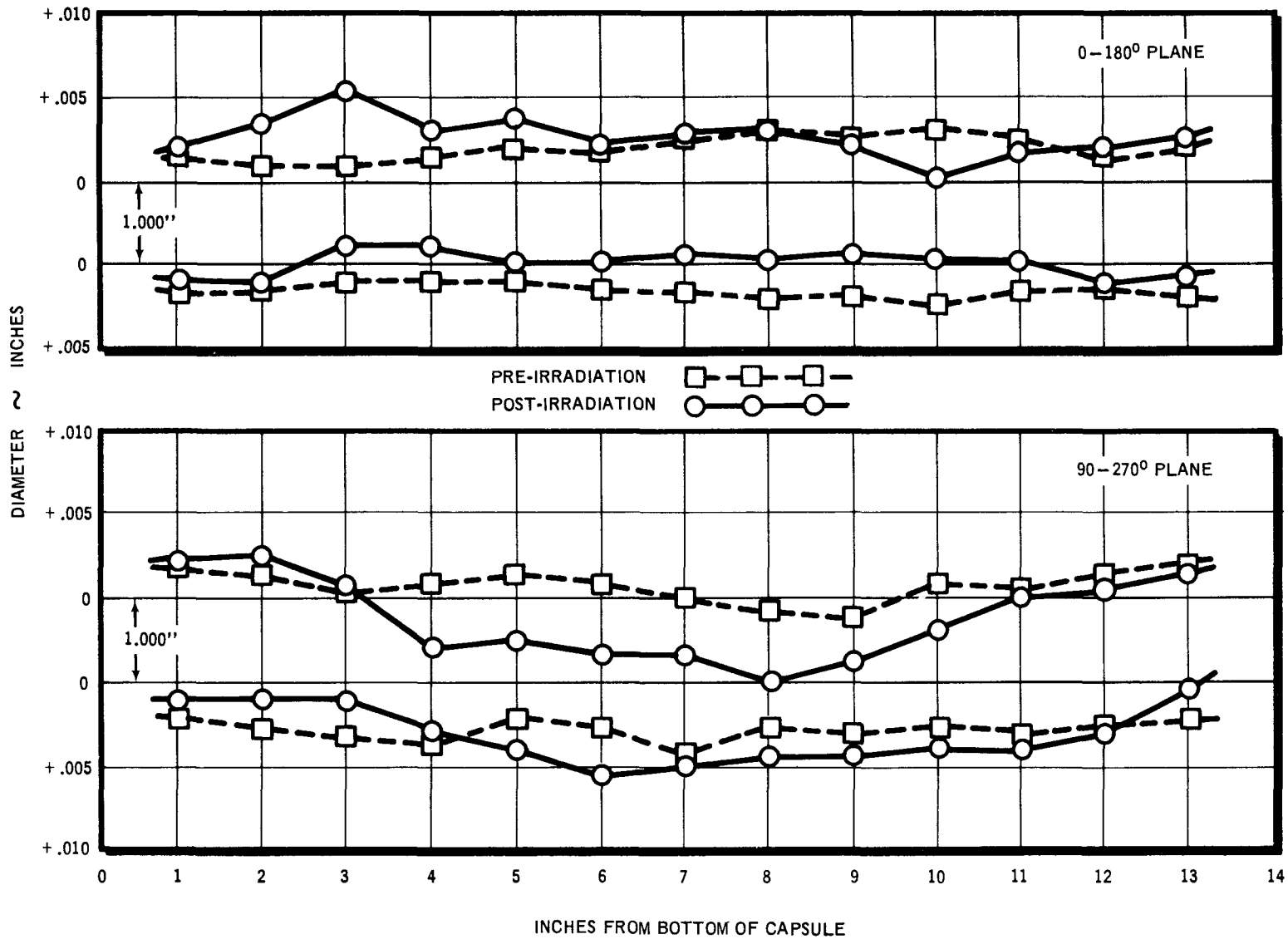

FIGURE 3 TREAT FUEL SAMPLE NO 1B, PRE AND POST IRRADIATION PROFILE MEASUREMENTS

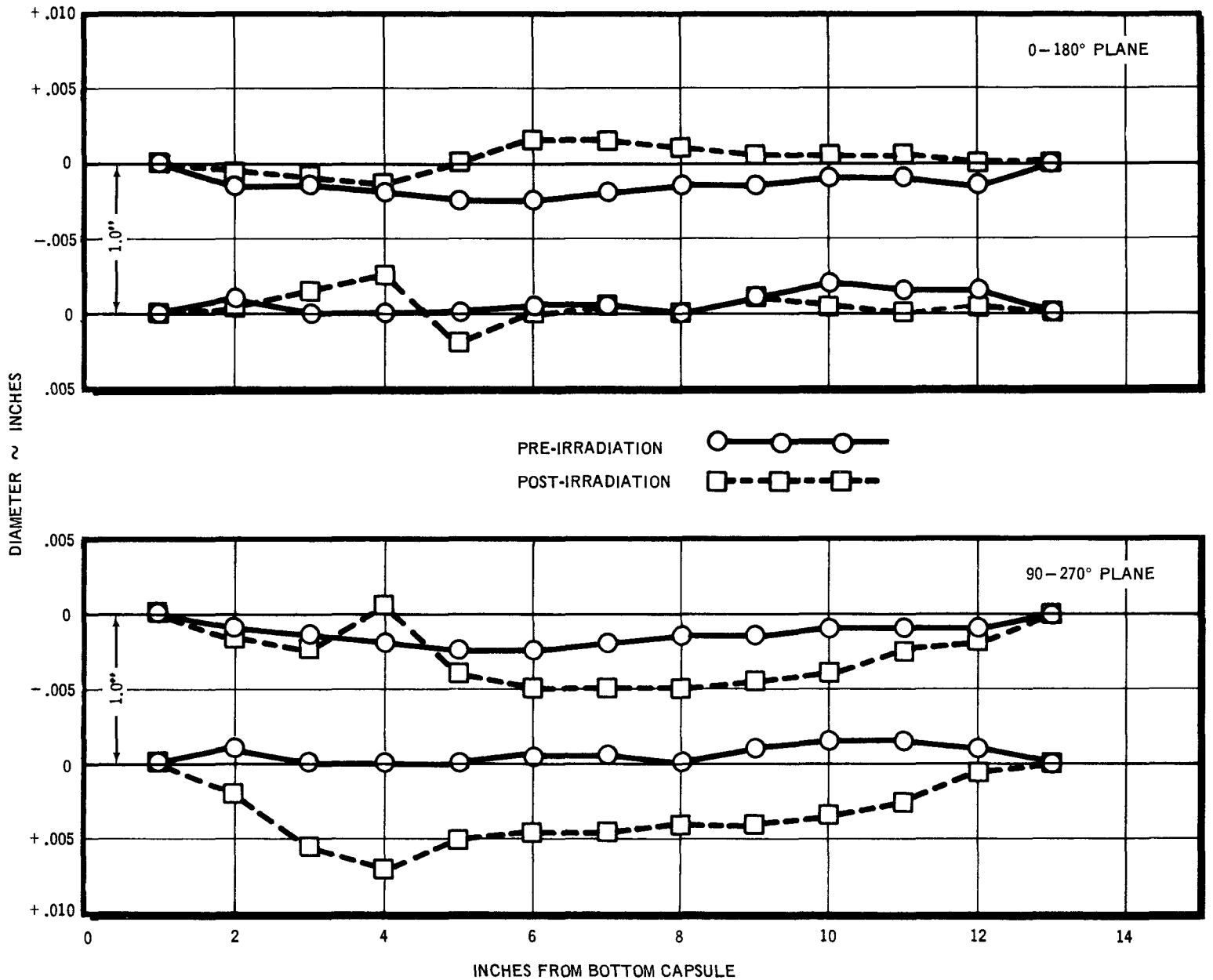

FIGURE 4 TREAT FUEL SAMPLE NO. IC
PRE AND POST IRRADIATION PROFILE MEASUREMENTS

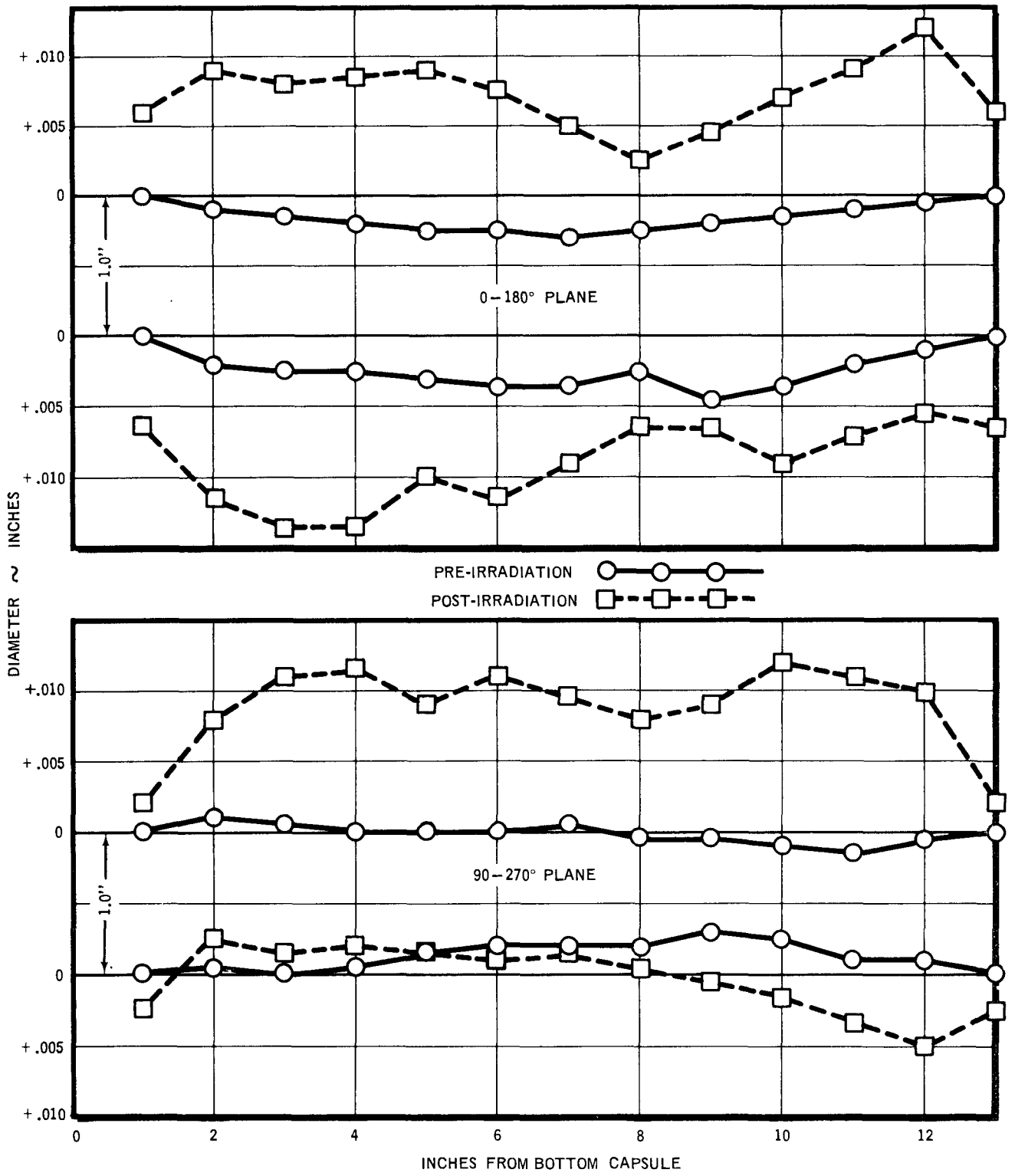

FIGURE 5 TREAT FUEL SAMPLE NO. ID
PRE AND POST IRRADIATION PROFILE MEASUREMENTS

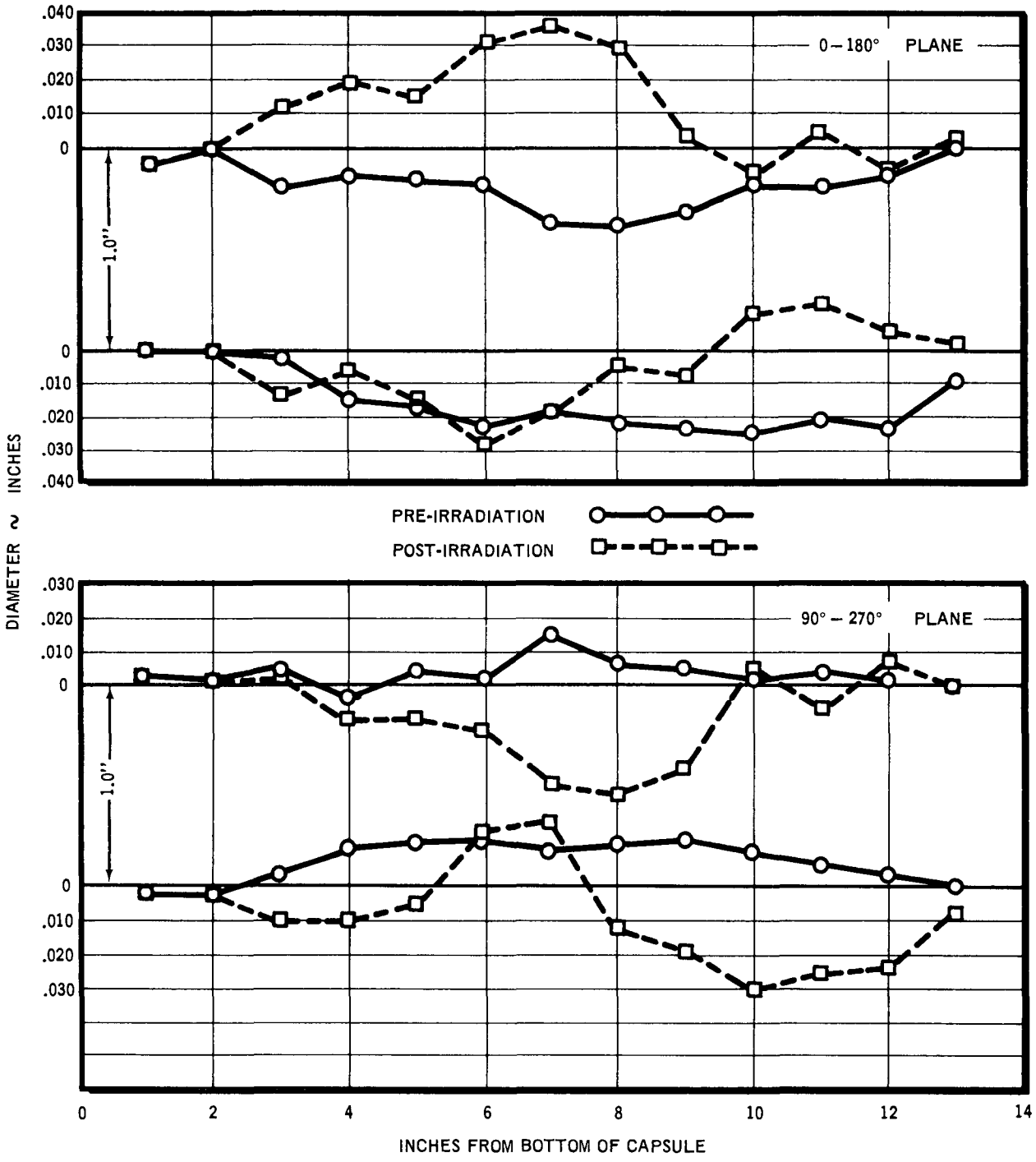

FIGURE 6 TREAT FUEL SAMPLE NO 1E
PRE AND POST IRRADIATION PROFILE MEASUREMENTS

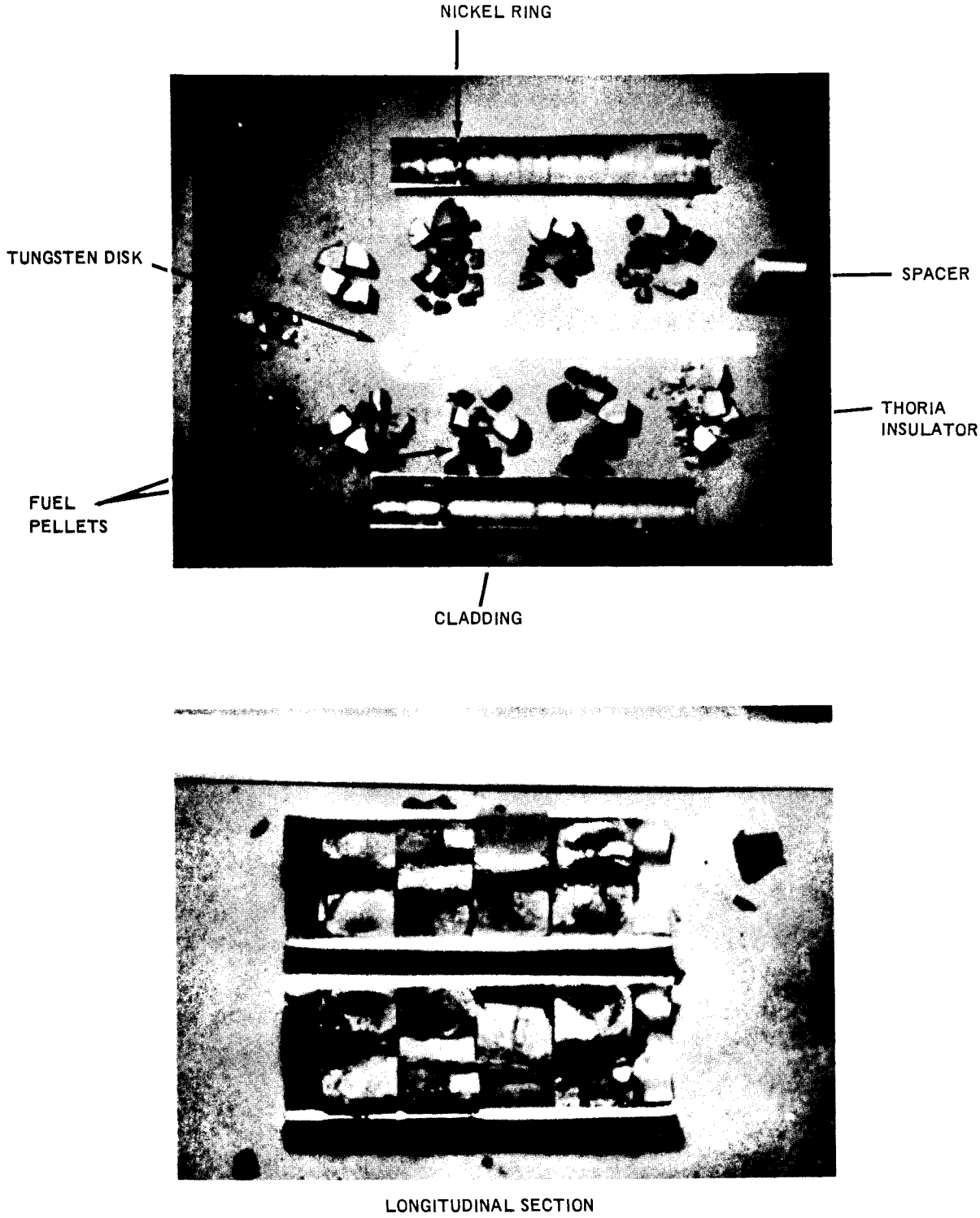

FIGURE 7 SAMPLE 1B, FUEL AND CLADDING INTERIOR

Void areas were formed throughout the fuel, varying from small, spherical pockets to a large central area extending the full length of the uppermost fuel section (see Figure 8). Pellet interfaces were no longer discernable and all fabricated gaps in the fuel area (both axial and radial) were filled with UO_2. Also noted were the characteristic columnar grains radiating from an incipient central void and the circumferential cracking near the fuel-clad interface. The tungsten support disks were bowed and pushed upward and it appeared that there were holes melted through at least one of the disks. Despite these indications of extremely high temperature, however, the interior surface of the cladding appeared undamaged.

Preliminary examination of specimen No. 1E revealed an incipient central void formation, but no columnar grain structure. It is apparent from the transverse sections shown in Figure 9 that the cladding was severely distorted in most fuel bearing sections. The UO_2 fuel section had the appearance of a polycrystalline mass with no columnar grains apparent in the macrostructure. In certain cross-sections, some central void was evident. The top section of the capsule from pellet 13 on was slit longitudinally and then split in half to expose the irregularity and the intermittent nature of the central voids. It was readily apparent from photographs of the inside surface of the cladding, that the large fragments of the fuel pellets were responsible for the undulation and protuberances in the stainless steel cladding. There was a direct correspondence between the crack pattern on the pellet surface and that on the inside surface of the cladding. Evidence of melting in the nickel ring was noted indicating improved thermal contact with the fuel due to the repeated transients. The tungsten disks appeared to have been fractured during the transients and were difficult to locate in the longitudinal sections.

6.3 Metallographic Examination

Transverse and longitudinal sections from each fuel sample were polished and etched for metallographic examination. Detailed study of these samples under high magnification revealed a logical progression in the appearance of the irradiated fuel, with increased transient severity. This progression was indicated in Table VI-1 at the beginning of the section summarizing the metallographic and other post-irradiation findings for all five samples in Series I.

Figures 10 through 12 are transverse sections of the first three samples at approximately 6 × magnification. These samples are very similar with the exception of very slight grain growth in specimen No. 1B and extensive grain growth in specimen No. 1C. In the latter sample, a region of sintering or fusion at one of the pellet interfaces was also noted (see Figure 13).

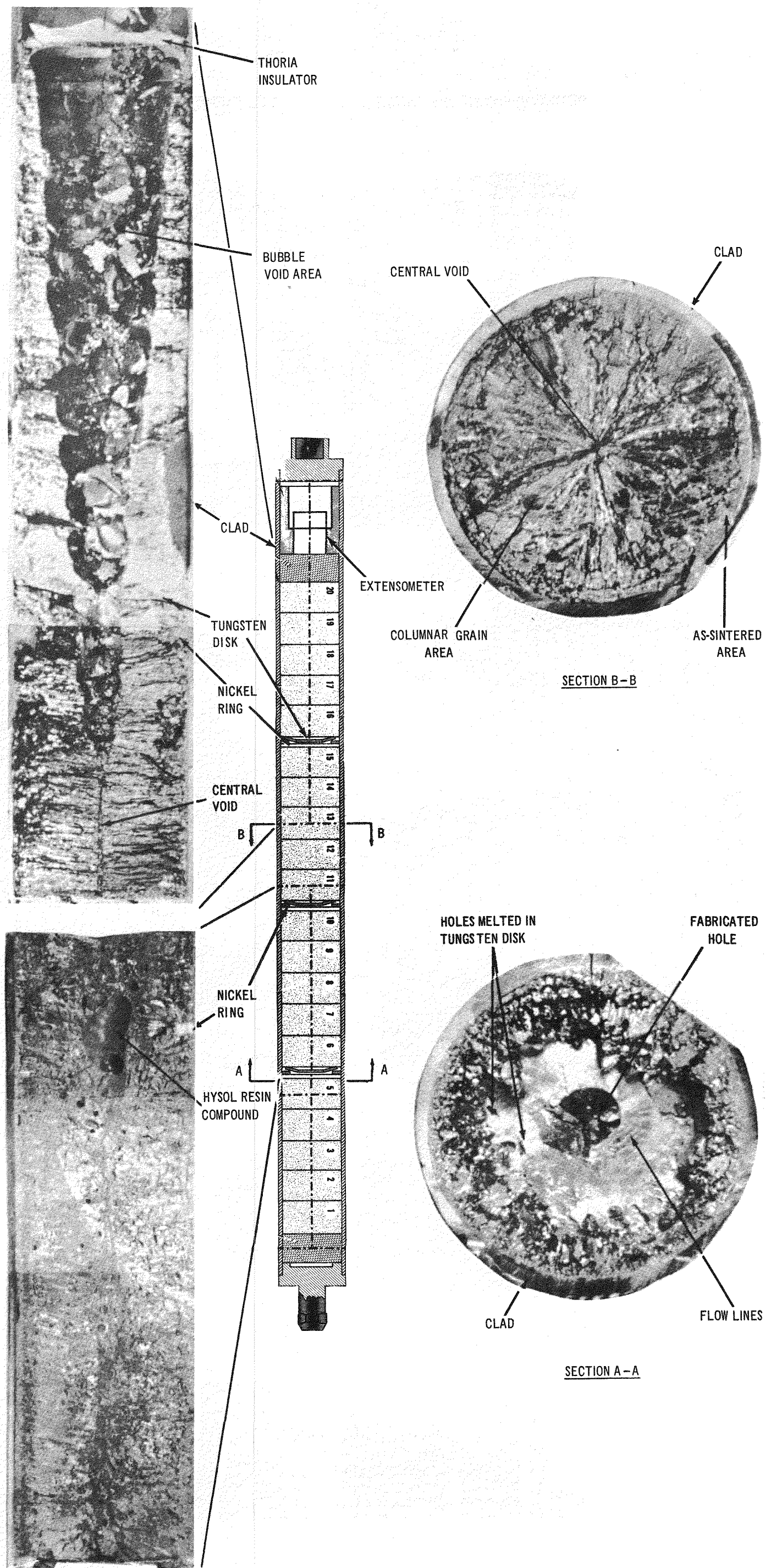

FIGURE 8 POST IRRADIATION SECTIONING OF SAMPLE 1D

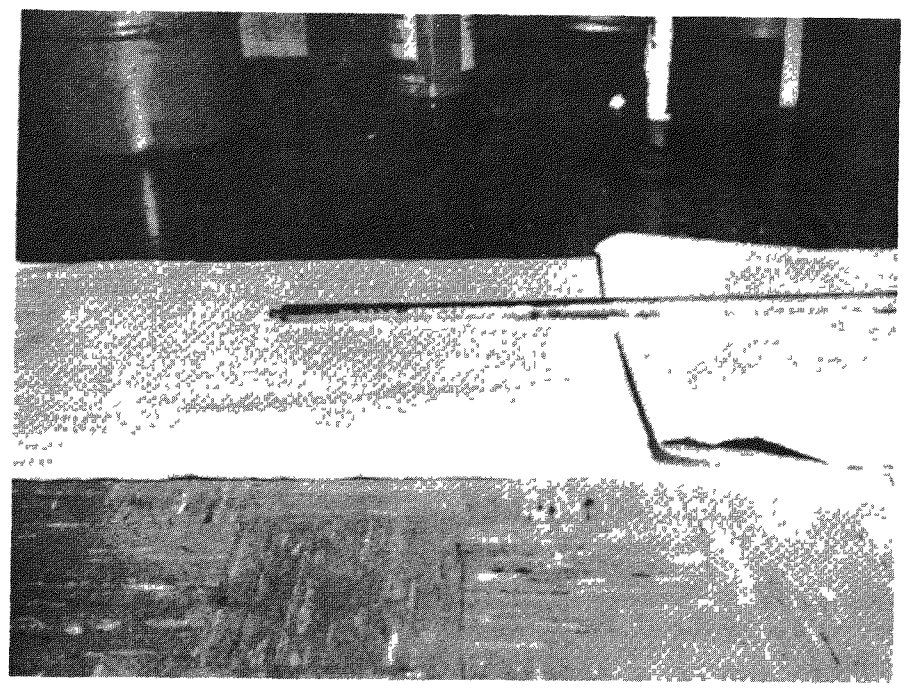

FUEL SPECIMEN AS REMOVED FROM CAPSULE

REMAINS OF TUNGSTEN DISK

CLAD

FUEL

PORTION OF NICKEL RING

TRANSVERSE SECTION

VOID AREA

ORIGINAL PELLET INTERFACES

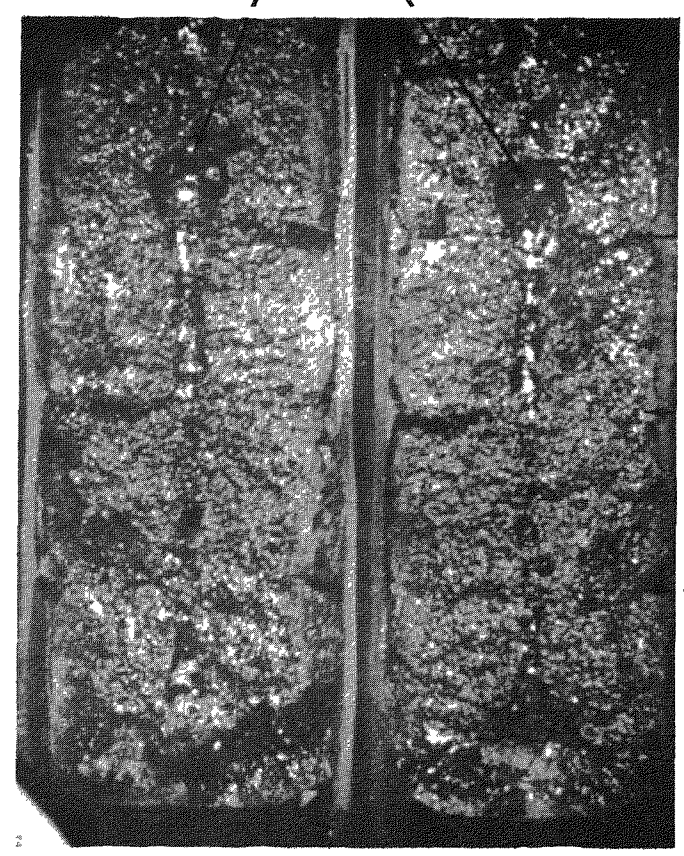

LONGITUDINAL SECTION

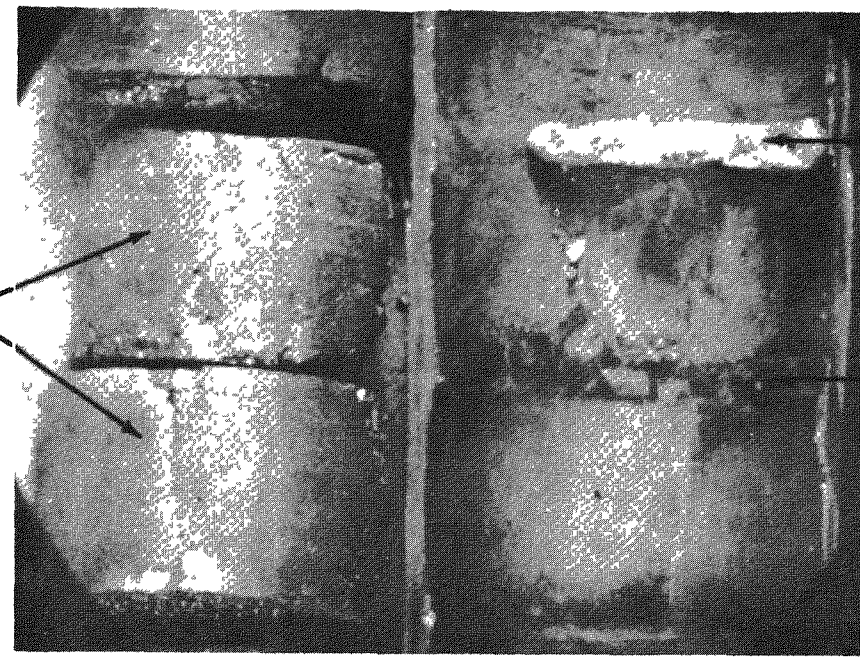

REMAINS OF MELTED NICKEL RING

CORRESPONDING FUEL PELLETS (EXTERIOR SURFACES)

CLADDING INTERIOR

FUEL REMOVED FROM CLADDING

FIGURE 9 POST IRRADIATION SECTIONING OF SAMPLE 1E

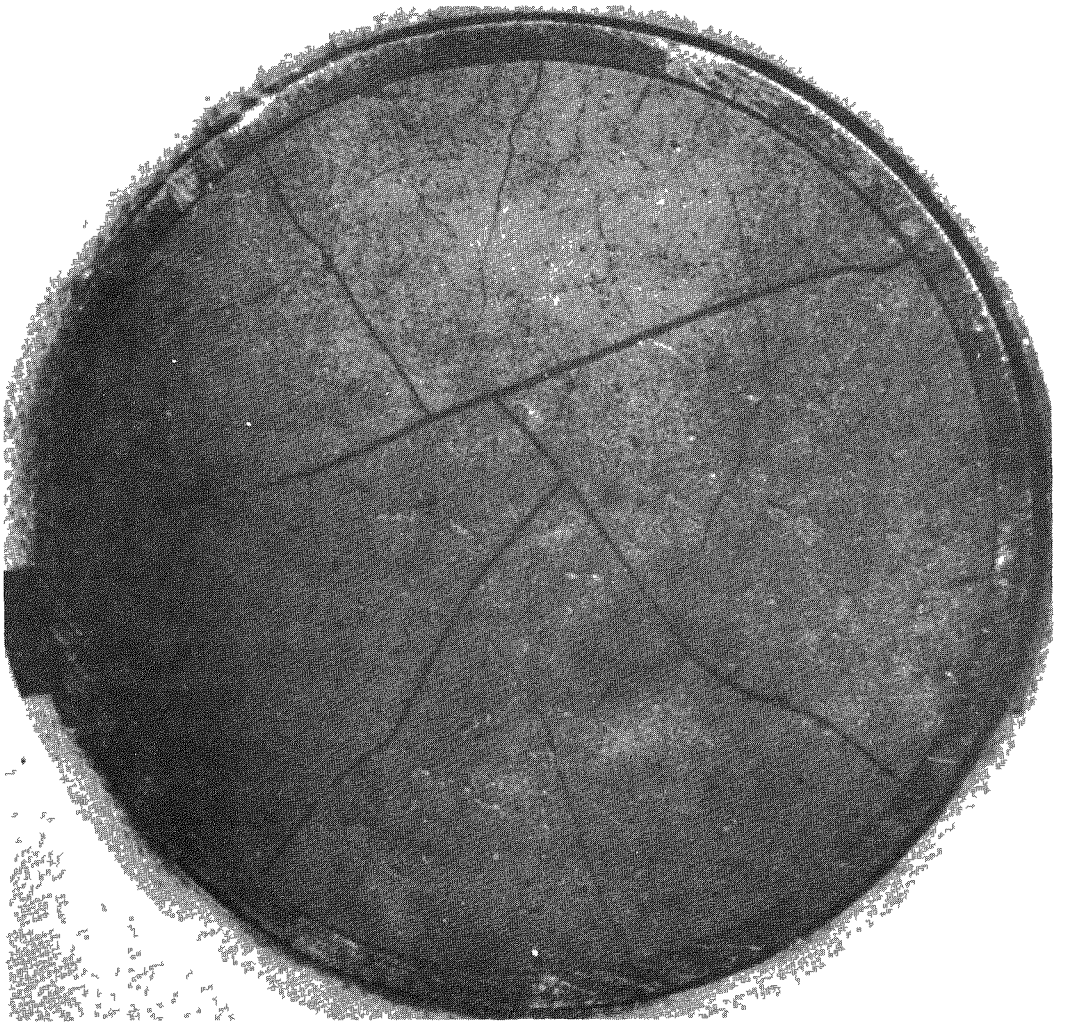

POST IRRADIATION TRANSVERSE SECTION

TREAT TRANSIENT POWER: 315 MW-SECONDS
GENERATED SAMPLE POWER: 136 ± 6 BTU/IN^3
ESTIMATED PEAK TEMPERATURE: 4090 ± 140 °F

FIGURE 10 APED–TREAT FUEL PIN NO. 1A

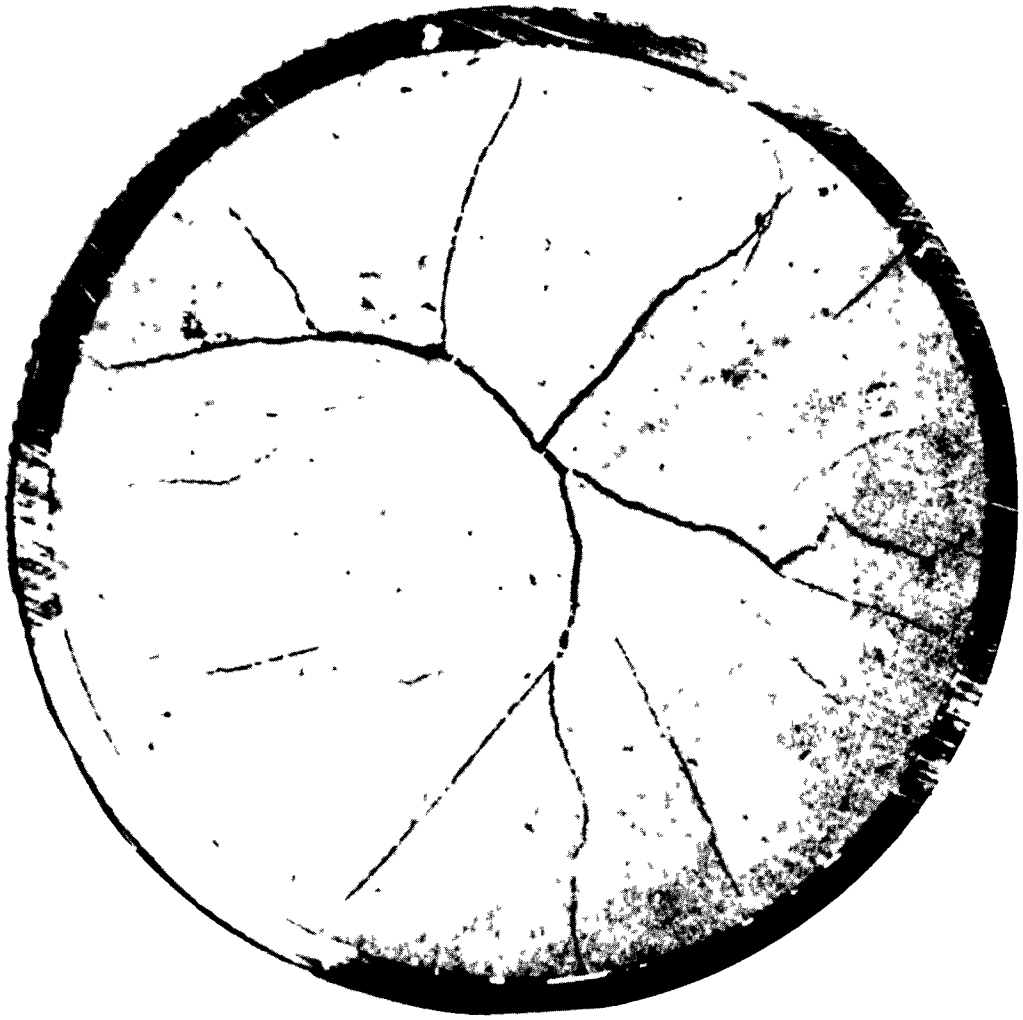

POST IRRADIATION TRANSVERSE SECTION

TREAT TRANSIENT POWER: 420 MW-SECONDS
GENERATED SAMPLE POWER: 190 ± 7 BTU/IN^3
ESTIMATED PEAK TEMPERATURE: 5000 ^{o}F

FIGURE 11 APED-TREAT FUEL PIN NO. 1B

POST IRRADIATION TRANSVERSE SECTION

TREAT TRANSIENT POWER· 520 MW-SECONDS
GENERATED SAMPLE POWER· 238 ± 10 BTU/IN^3
ESTIMATED PEAK TEMPERATURE: 5220 ± 210 °F

FIGURE 12 APED–TREAT FUEL PIN NO. 1C

Metallographic longitudinal sections of sample No. 1D are shown in Figures 14 and 15. From a study of these and other photomicrographs, it was observed that the large columnar grains extended radially outward to about 95 per cent of the pellet radius. The UO_2 grain structure in this region appeared to be very dense and porous both within the columnar grains and in the grain boundaries. Smaller columnar grains were present in the zone from about 85 per cent to 95 per cent of the pellet radius. Some large radial cracks were observed throughout the region of columnar grain growth. The density and the extensive columnar grain growth, resulting from one transient in TREAT, suggest that this region in the pellet was molten. The observed structure probably resulted from the solidification of the molten material as heat was transferred radially to the cladding. The remaining 5 per cent of the radius consisted of an outer rim of UO_2 which retained its fine-grained, equiaxed, "as-sintered" structure, and a narrow zone showing equiaxed grain growth and the transition to columnar grain growth. Detailed examination disclosed that this outer rim did not melt during the irradiation, but that it did crack, probably from the thermal stress or expansion of the molten core. Molten UO_2 from the interior of the pellet penetrated some of the larger cracks, and in at least one instance flowed into the gap between the pellet surface and the stainless steel cladding (see Figure 16). The solidified structure was observed as "fingers" of UO_2 having dense columnar grains which formed a continuous structure with the previously molten core material. Some of these cracks also contained a metallic constituent which was present in relatively large masses and appeared distinctly separate from the solidified urania fingers. Since this metal phase was readily etched with the urania, and was found to be optically active under polarized light, it was tentatively identified as uranium. Hardness tests were conducted on one of the largest samples of this metal phase, and it was indicated that it was a relatively soft material (i.e., not stainless steel). One particularly large piece of metallic phase material was isolated and placed in the powdercamera, however, it was identified as nickel. Thus, the identity of this metallic phase or phases is still in doubt and requires further investigation.

One transverse section of sample No. 1E was prepared for metallographic examination (see Figure 17). This section clearly shows the distortion of both fuel pellet and cladding and indicates extensive equiaxed grain growth over most of the pellet, but no columnar grains. It appeared that the outer edge of the fuel pellet remained in the "as sintered" condition and did not become plastic during the irradiation. It is significant to note that the radius of curvature of most segments of this outer crust was found to be less than the original "as fabricated" pellet radius.

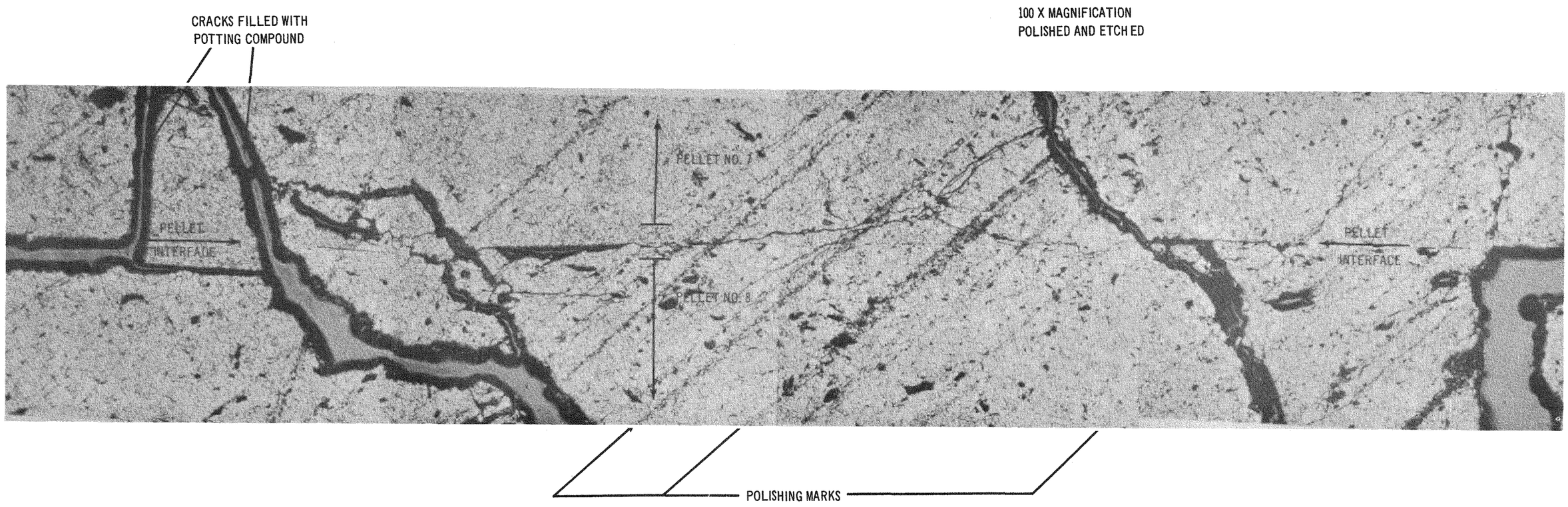

FIGURE 13 SAMPLE 1C, FUSION OF PELLET INTERFACES

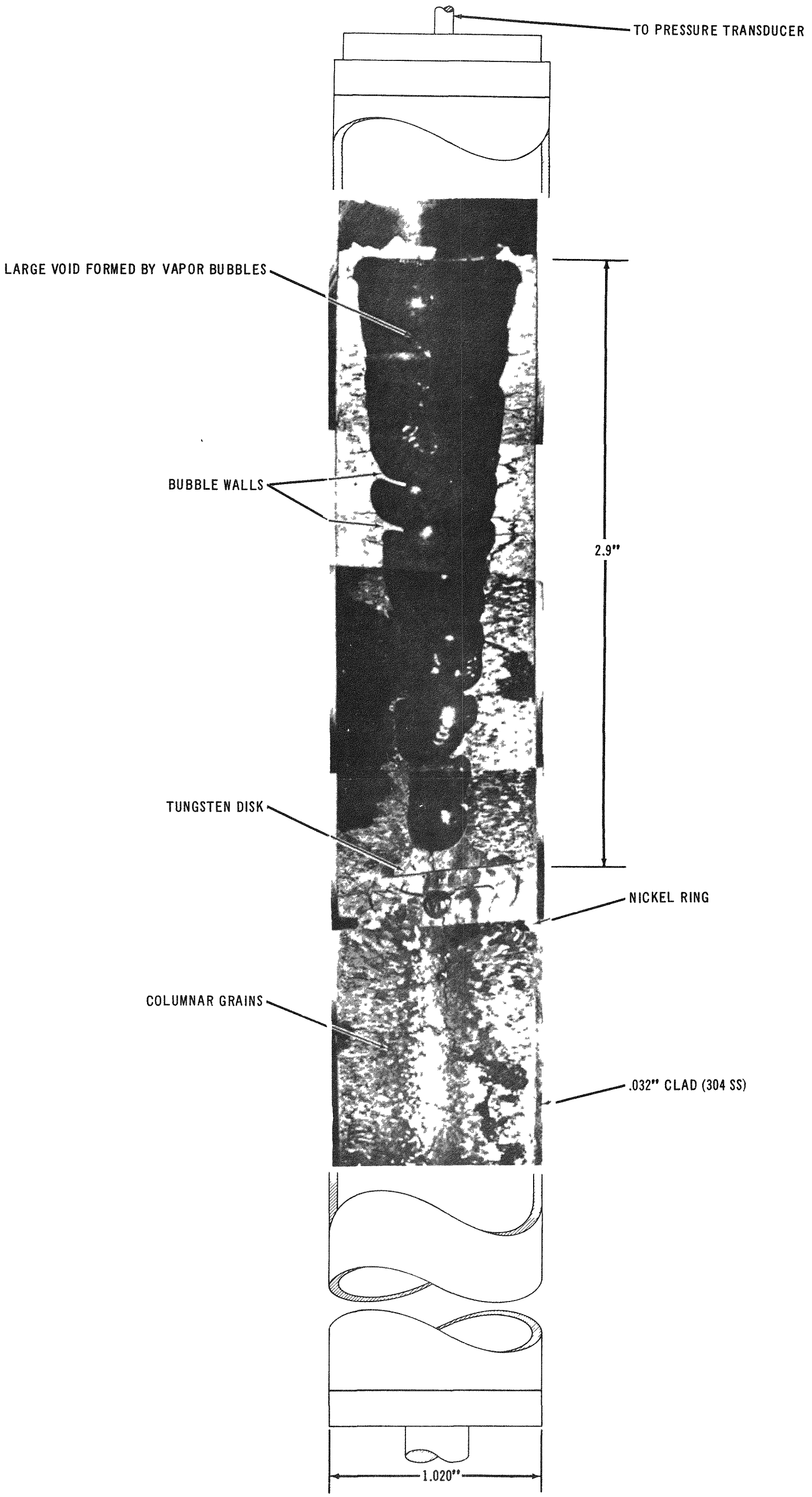

FIGURE 14 UPPER SECTION APED-TREAT SAMPLE 1D

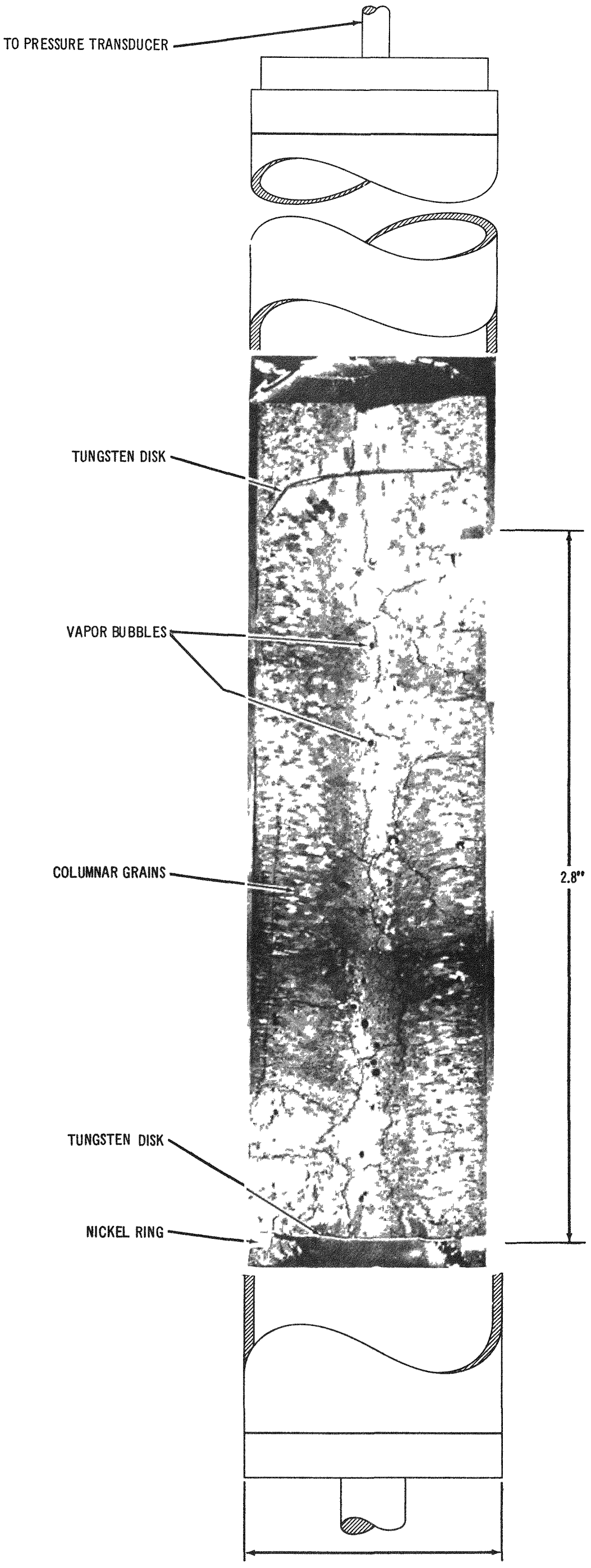

FIGURE 15 CENTRAL SECTION APED-TREAT SAMPLE 1D

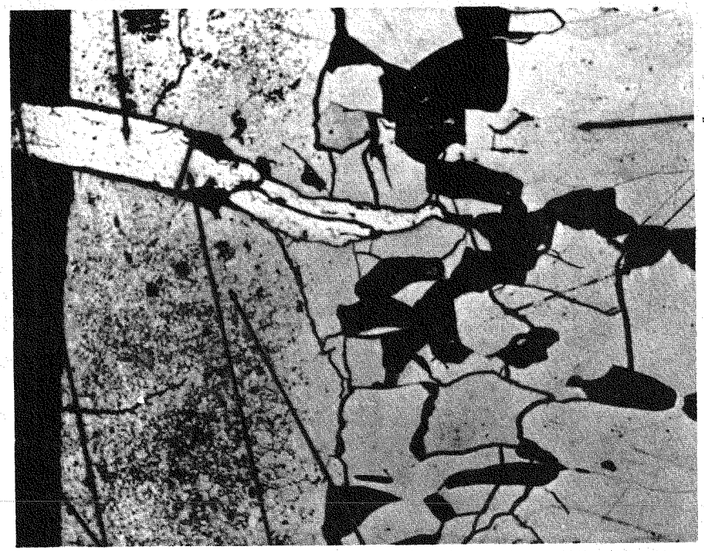

SAME AREA

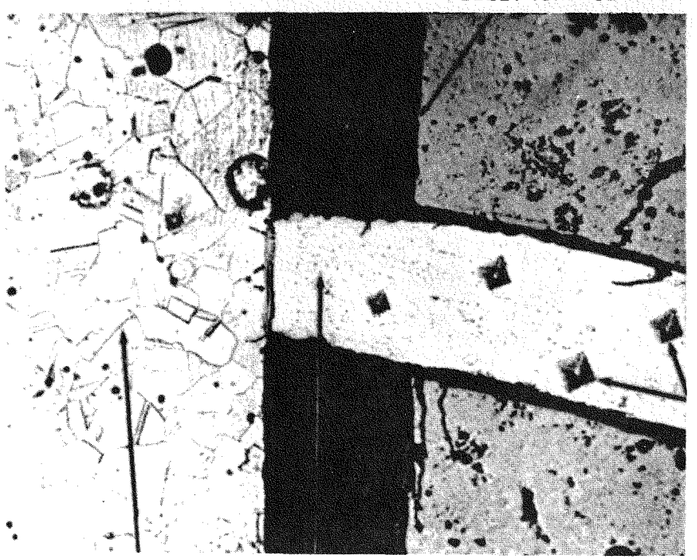

FIGURE 16 PHOTOMICROGRAPHS OF FUEL-CLAD INTERFACE – SAMPLE NO. 1D

736-16

FIGURE 17 SAMPLE NO. 1E POLISHED CROSS SECTION

SECTION VII

DISCUSSION OF RESULTS

As previously stated and shown in Table VI-1, there was a logical progression in the appearance of the irradiated fuel with increased transient size. The first effect to become evident was radial cracking of the fuel pellets, which was seen to grow more severe as transient size increased. There appeared to be some indication in sample No. 1C that the pellet center cracking was a result of oxide fuel shrinkage in that region. This conclusion was strengthened by a slightly dished appearance at the pellet interfaces which was not noted in the un-irradiated control sample.

There was evidence of inelastic expansion of the fuel pellets in all cases with utilization of the expansion spaces provided. The extensometers in the last three specimens (see Section 4.1) indicate a greater expansion had occurred than would be expected on the basis of published expansion data [12] for solid UO_2 - a portion of the fuel was estimated to be in excess of the melting point. This could be due to a number of effects; such as phase change expansion (~10 per cent), * violent rupture of the intervening thoria insulator under severe thermal gradient, vapor pressure (sample No. 1D), or simply handling effects. The extensometer in sample No. 1E (repeated transients) showed only the effect of the first transient indicating that further axial expansion was transfered to the cladding.

Grain growth was noted in all but the first sample irradiated. It is believed that the fuel in this initial specimen was above its sintering temperature for too short a time to permit grain growth. No attempt has been made to correlate grain size with estimated temperatures other than to observe that the number and size of the enlarged grains increased with transient size. A more rigorous correlation would be difficult since grain growth has a time-temperature dependance and the time parameter for these tests is well below that found in the literature. [13]

Void formation in the irradiated fuel was limited to the last two specimens (No. 1D and No. 1E). In the former case, most voids take the shape of bubbles, apparently due to a boiling phenomenon. Large bubbles in the upper section were apparently separated by menisci, while more finely dispersed

*(7.2 per cent) as reported in a paper presented to the 15th Pacific Coast Regional Meeting of the American Ceramic Society, Oct. 17-19, 1962; "Specific Volume of Molten UO2", J. A. Christiansen, HLO

bubbles were found throughout the high temperature section. An annulus of small bubbles was evident in this sample (1D) near the outer radius, (see Figure 15) indicating a transient temperature spike in this region as expected from flux depression considerations.

Finely dispersed bubbles were again noted in sample No. 1E with the heaviest concentration near the pin center. The incipient characteristics of a normal central void formation were also apparent as was the case in the central section of sample No. 1D. It appeared that only the outer edge of the fuel pellet remained in its "as sintered" condition and did not become plastic during the course of irradiation. In some areas fusion has occurred between the UO_2 pellets, thus closing the cracks in the center region. The warping of the outer crust of each pellet segment was probably due to the contraction of its center while cooling.

The appearance of the metallic phase in sample No. 1D gives rise to speculation concerning the possible disassociation of UO_2 at elevated temperatures. The oxygen thus released could result in oxidation of internal components or might contribute to transient pressure levels.

It should be emphasized that the cladding maintained its integrity (did not rupture) in any tests in the series, and in fact was undamaged with the exception of the deformation in the most severe experiments. This performance is impressive in view of the extreme temperatures involved as evidenced by the melting of the nickel rings (~2650 F) attached to the clad, and in some locations melting of the tungsten disks (~6100 F).

7.1 Postulated Sequence of Events in Power Transient

7.1.1 The neutron pulse supplied by the test reactor causes a release of energy from a portion of the fissile material present in the fuel. (The flux depression fequently present in the fuel results in maximum energy release at the fuel surface).

7.1.2 Fission fragments having a mean path length in UO_2 of ~5 microns deposit energy in surrounding fuel material (fission product spikes). This rise in energy content of the fuel is approximately uniform across the entire cross section of fuel save for the effects of flux depression. It is superimposed on the previously existing temperature profile in the fuel (Flat with no preceeding power generation, otherwise approximately parabolic).

7.1.3 The rise in energy content of the fuel is evidenced as an equivalent rise in fuel temperature, tempered by the effects of: -

- variable specific heat
- latent heat of fusion when MPt is reached
- latent heat of vaporization
- heat of dissociation, etc.

7.1.4 The transient increases in fuel temperature result in the following: -

- heat flow from the hottest fuel to the clad and sometimes also toward the fuel centerline due to flux depression effects.
- a tendency for fuel volume increase due to thermal expansion, liquefaction, vaporization, or gas release.
- the generation of thermal stresses in the fuel itself and accompanying or subsequent cracking.
- possible changes in chemical equilibrium between fuel and gas phase, etc.

7.1.5 The rates of heat flow to the fuel clad and in consequence the temperature gradients in the fuel clad can be extreme and result in thermal stresses well beyond the yield point. Such occurrences were considered in some detail in reference (1) and appear consistent with finding in the present experiments. Therefore they are not considered further here save to say that heat flow and thermal stresses per se should not (and did not) result in rupture of the fuel clad providing it remains in a ductile state and is adequately cooled externally.

7.1.6 Effects of volume increases in the fuel although alluded to in the preceding analytical study cannot be computed effectively. They have, however, shown up as one of the major effects causing fuel deformation in the present series of tests.

7.1.7 In the absence of restraint the fuel will expand freely as a result of the factors listed above. In practice some degree of restraint is always present frequently from the clad and even from within the fuel itself; the cooler regions of the fuel tend to restrain expansion of the hotter central regions. This restraint of the fuel has been observed on many occasions to result in plastic flow of hot material and in the case of fuel of less than theoretical density

(internal voidage) compression or collapse of the voids is also possible. Such plastic flow is time, temperature and pressure dependent and as such will be more evident in the hottest regions of the fuel, particularly in prolonged transients. (It is in fact directly akin to the sintering process.)

Plastic flow and densification (sintering) of the fuel during transients is clearly evidenced in the present series of tests in at least three cases, namely: -

Figure 14; where "extrusion" of the fuel past the nickel ring in test 1D due to extreme volumetric expansion of the fuel body carried the tungsten disk ahead of it.

Figure 9 where a distinct barrel shape is evident in the fuel pellets which were originally centerless ground. This is believed due to compaction of the hot central cylindrical portion of the fuel which on subsequent cooling would tend to pull the fuel into the barrel shape. Figure 17 where the radius of curvature of the fuel pellet surface following transient test 1E is significantly less than in the "as fabricated" condition and less than that of the clad within which it was contained.

7.1.8 The time, temperature and pressure dependence of the plastic flow implies that during a given transient the fuel will expand as its temperature rises at a rate approaching that of unrestrained expansion until such time as the fuel-clad gap is taken up and the clad or its equivalent is contacted. At that point the initial limited restraint due to the cooler regions of fuel acting in tension will be re-inforced by whatever strength the clad possesses.

7.1.9 Given sufficient clad strength and sufficient plasticity and void content in the fuel there is evidence that further fuel expansion can be prevented.

7.1.10 In the absence of such conditions further expansion of the fuel at a reduced rate is to be expected and will be accompanied by elastic then plastic deformation of the clad. (This will also be accompanied by improved heat transfer between fuel and clad.)

7.1.11 Plastic deformation of the clad will result in binding at fuel-clad interfaces with respect to relative translational movement and in consequence will tend to produce longitudinal stretching of the clad regardless of the presence or absence of longitudinal expansion spaces. (This occurrence is evidenced in test 1E.)

7.1.12 For very rapid rates of power input as would occur in a prompt power excursion in EFCR, for instance, there will be a negligible time period available for plastic flow and in consequence even the hottest UO_2 will tend to act as a rigid solid, thus producing maximum clad deformation.

7.1.13 Continued energy input to the fuel beyond that necessary to take the fuel to its melting point will result in melting of the fuel with no temperature increase in the melting zone until such time as the full latent heat of fusion has been absorbed.

7.1.14 The large volume increase (~10 per cent) associated with melting will give rise to significant local pressure generation and fuel movement during a transient and this is evidenced in test 1D (Figure 16) by the presence of rapidly chilled UO_2, apparently extruded in its molten state into the cracks in cooler unmelted material adjacent to the clad.

7.1.15 Additional fuel movement due to slumping or draining of the molten UO_2 will also tend to occur and may be evidenced in test 1D (Figure 14).

7.1.16 Still further energy input to the fuel beyond melting will raise its temperature to levels at which its vapor pressure becomes appreciable. Considerable uncertainty exists on the composition of the vapor which will be in equilibrium with high temperature UO_2, however some degree of thermal decomposition is quite probable. Under circumstances in which some portions of the fuel material are hot enough to exert a vapor pressure in excess of the prevailing pressure in the capsule then boiling is to be expected and will result in vapor voids opening up within the liquid fuel mass, thus expelling it to lower pressure (cooler) regions. This is evidenced in test 1D (Figure 8) where the upper end leads to the pressure sensor (a volume sink).

7.1.17 Still further energy input can be expected to generate sufficient pressure and energy of expulsion to cause bursting of the fuel pin.

7.1.18 Any magnitude of power transient that results in non-elastic deformation to the clad and damage (cracking, etc.) of the fuel may with repetition give rise to ratcheting

phenomena and thus to progressive damage. This results from the fact that, in the case of non-elastic deformation, the fuel does not return to its original configuration following a transient, e.g.,

The fuel cracks and tends to move outward thus filling the initial fuel-clad expansion space (see Figure 12).

The clad when stretched beyond its elastic limit will stay in its extended state.

The fuel may tend to sinter thus generating a central void and high density material in contact with the now extended clad. (See Figure 8.)

SECTION VIII

RECOMMENDATIONS

8.0 General

On the basis of experiments carried out to date it appears that unirradiated stainless steel clad oxide fuel of the type proposed for EFCR and FCR can withstand a single power transient which results in maximum fuel temperatures approaching 7000 F, provided adequate cooling of the cladding is available. Beyond this point rupture of the clad due to internal pressure generation is anticipated. In the absence of effective cooling, excessive clad temperature (1,800 F) and a consequent premature failure is to be expected.

8.1 EFCR Fuel

Multiple transients of interest for EFCR experiments, appear to give rise to progressive fuel damage due to what might be termed a ratcheting phenomenon. There is, however, some hope that this may be minimized or eliminated in an EFCR type fuel by suitable design, namely, very strong clad capable of restraining the fuel, coupled with use of fuel containing sufficient void (central core ultimately) to accommodate all the volumetric expansion anticipated.

8.2 FCR Fuel

For FCR fuels, the above (8.1) provisions are unnecessary as severe transients are considered a "once-in-a-lifetime" incident. Thus, single transient performance limits are of prime interest.

Further studies of performance limits of fast ceramic reactor fuel are recommended and planned [14] to cover effects of: -

a. Use of mixed oxides

b. Smaller fuel pin diameters

c. Presence of fission products, and absence of "as fabricated" fuel-clad gap and possible irradiation hardening and thermal conductivity changes in preirradiated fuel.

8.3 Test Facilities

A fast transient test facility, "F-TREAT", appears to be very desirable for future development of fast reactor fuels if transient performance continues to be a major interest. In view of the suspected significance of plastic flow phenomena on fuel damage, transient power generation rates comparable with those of a fast excursion are necessary. (TREAT transient times and thus the available period for plastic flow are one to two order of magnitude greater.) The presence of a flux depression using the TREAT (thermal facility) precludes testing of a prototype fast reactor fuel assembly and thus studying possible pin interactions. Also, flux depression effects even in a single pin containing a representative plutonium content can have a significant influence on its performance.

SECTION IX

ACKNOWLEDGEMENTS

Fuel test specimens were fabricated in the Fuel and Materials Laboratory, APED, San Jose by J. T. Mommsen and J. J. McCoy.

Capsule design was done by J. H. Germer and E. O. Winkler and fabrication accomplished at Vallecitos Atomic Laboratory by J. E. Hanson and W. J. Vahlensiech.

Testing was performed in the ANL-TREAT facility by Messrs:

J. F. Boland - Manager, TREAT
F. S. Kirn
H. Lawroski
R. DeForest

R. M. L. examinations and analysis were carried out at Vallecitos Atomic Laboratory by R. C. Nelson and J. M. Gerhart

APPENDIX A

TREAT CAPSULE DESIGN

In order to accomplish the planned irradiation in TREAT, it was necessary to construct test capsules to contain the fuel sample within the reactor core. A new capsule was assembled for each test with some undamaged parts being reused when activity levels permitted.

Capsule Criteria

The conceptual design of the TREAT test capsule was based upon the need to satisfy several criteria:

a. In order to be placed within the TREAT core for testing, the capsule must fit within the space provided for a single TREAT fuel element.[6] Thus, the exterior of the capsules was dimensionally the same as a TREAT fuel element with the exception that the central portion was cylindrical instead of square. The upper and lower ends were square to provide alignment with surrounding fuel elements (see Figure 18).

b. It was desired that the capsule be capable of rapid dissipation of the heat generated in the fuel in order to provide a good simulation of the radial temperature profiles expected in EFCR. In addition, it was necessary that the capsule absorb all of the heat generated in the fuel during a transient without rising to temperatures in excess of those expected in the experimental reactor. These objectives were satisfied by surrounding the fuel pin with a large beryllium heat sink, thermally bonded to the sample with a small annulus of sodium.

c. In order to provide an accurate estimate of the total transient energy release of the test specimen, it was necessary for the capsule to act as a calorimeter. Thus, the inner capsule, containing the heat sink, was insulated from the outer can and the heat path to the upper end piece was kept to a minimum.

d. It was also necessary that the capsule have the capability to withstand internal pressures generated in the course of planned experiments or in possible accident situations. In addition, containment was needed for fission products as well as sodium or other materials

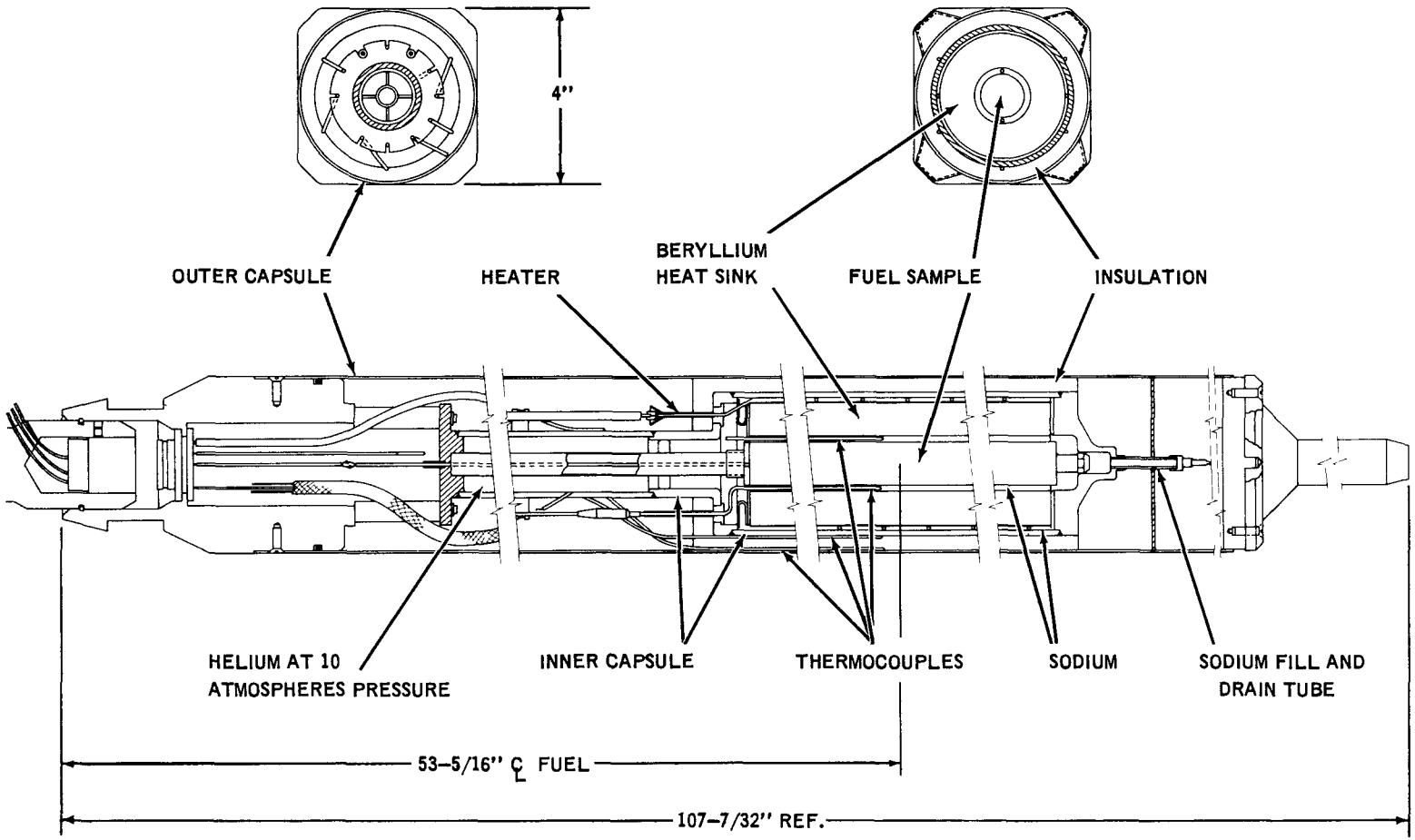

FIGURE 18 SERIES 1 TREAT CAPSULE

which might cause chemical reactions in the TREAT core. In view of this, all inner capsule joints were welded and each capsule was required to be helium mass-spectrometer leak tight.

e. Since it was not considered feasible to initiate transients with a fuel temperature regime similar to EFCR operating conditions, it was decided that fuel cladding temperatures could at least be simulated by starting from the reactor coolant outlet temperature of 800 F. For this purpose, externally controlled heaters were installed in the sodium annulus just outside of the beryllium heat sink.

A detailed description of the capsule design and fabrication as well as a discussion of significant capabilities of the assembled test apparatus, has been included in the Hazards Analysis and Test Specifications for Series I. [15, 8] Table A-1 is a summary of pertinent capsule and fuel pin parameters which were calculated and/or measured prior to and during the test series.

TABLE A-1

SUMMARY OF SERIES I TEST APPARATUS CHARACTERISTICS

Internal pressure capabilities: (Calculated)

Fuel pin - yield pressure = 1330 psi at 900°F

- burst pressure (radially) = 3870 psi at 900°F

(axially) = 7740 psi at 900°F

Inner capsule - yield pressure = 1800 psi at 800°F

= 1380 psi at 1200°F

- burst pressure = 5200 psi at 800°F

(fuel pin burst pressures measured: 4400 psi at 800°F

9800 psi at rm. temp.)

Heat capacity of assembled capsule:

Calculated at 1000°F	4.6 BTU/°F
Measured at 750°F	4.5 BTU/°F
at 500°F	4.1 BTU/°F

Sample power ratio: (watt-sec/cc of sample energy per watt-sec of TREAT power)

Calculated $P_s = 2.0 \times 10^{-5} P_t$

Measured $P_s = 2.8 \pm 0.2 \times 10^{-5} P_t$

Radial power gradient due to self-shielding:

(calculated) 0.73

APPENDIX B

FUEL FABRICATION PROCEDURE

The fuel pellets used for this test series were fabricated by pressing uranium dioxide ceramic grade powder and sintering the pressed pellets in a hydrogen atmosphere to a density of approximately 95 per cent. Finished pellet lengths varied from 0.537 inch to 0.549 inch and diameters were ground to 0.922 inch on a centerless grinder. Thoria insulator pellets were made by the same procedure. Chemical analyses of the fuel material was made to determine enrichment, impurities and o/u ratio (see Table IV-1). A diamond grinding burr was used to grind holes in the required pellets for thermocouple capsule No. 1A. The diamond burr was rotated by a Dumore type sensitive drill press with the pellet contained in a cup-type fixture filled with water. The water helped contain the radioactive material and also served as a lubricant to prevent cracking. All pellets were dried after the grinding operation in a hot air furnace at 250 F for two hours.

All tubing was tested by ultrasonic methods to detect internal structural flaws, and found to be acceptable on the standard 10 per cent acceptance level (acceptable tubing may have structural flaws of up to 10 per cent of the thickness of the tubing). Burst tests were performed on "as received" tubing as well as on sections containing partition rings welded to the inside diameter. These tests showed essentially no loss of strength due to spot welding.[8] Tungsten and tantalum partition disks were cut to shape from sheet stock using a Dumore grinder mounted in a lathe tool post. The tungsten disks were dished at elevated temperature in order to retain the required angle of 5 degrees. A punch and die fixture was made for this purpose. Cobalt disks were fitted into a recess machined in the lower end plug. A size to size fit was established and the disks were staked into place using a sharp punch to displace material along the edge of the recess. Nickel partition rings 0.050 inch wide by 0.750 inch ID by 0.934 inch OD were spotwelded to the inside diameter of the stainless steel tubing using a Federal type resistance welder, (Press type - 30 KVA Mfg. type BAP-3-12S and P), equipped with a General Electric Sequence weld timer, plus a heat and slope control unit.

After cutting a piece of tubing to the desired length, the lower end plug was inert arc welded to the tube using a Miller DC welder with high frequency started and weld sequence timer.

Machine settings	- 54 amps DC
Gas flow	- 12 cfm Argon
Electrode	- 1/16 inch dia. 2 per cent thoriated tungsten.
Weld lathe speed	- 6 RPM

The tubing was then cleaned and the first stack of pellets inserted (1 thoria +5 UO_2). The length and weight of each group of pellets was recorded as assembled into the tube. A fixture was used to position the nickel ring the required distance (0.070 inch) above the uppermost pellet. This fixture was made of copper and also served as an internal electrode during spot welding. One end of this positioning rig was adjustable to serve as a stop for checking and measuring purposes. Following the weld, the fixture was used to check the location of the ring against a scribe mark on the outside of the tube. The partition disk was dropped into place atop the ring (dished downward) and the next compartment of pellets loaded on top of the partition disk. The measuring, marking, checking and welding steps were repeated for the remainder of the rings.

The required stainless steel filler plug, extensometer, or thermocouple was fitted to the capsule in preparation for vacuum outgassing, helium filling and final welding. The assembled fuel pin and end plug were placed in the weld chamber and the chamber evacuated to a pressure of less than one micron for a minimum period of three hours. The chamber was then back-filled with reactor grade helium and slowly lowered from approximately three pounds helium pressure to approximately one fourth pound helium pressure. The chamber doors were opened and, through glove ports, the end plug was assembled and welded to the tube. This final weld was made in a pure helium atmosphere. All fuel pins were mass spectrometer leak tested to a sensitivity of 10^{-8} cc per second and x-rays were taken to verify position of all internal components.

APPENDIX C

EXPERIMENTAL TECHNIQUES FOR TESTING AT TREAT

The procedure employed in each of the five tests making up Series I, were similar with the primary variable being the size and number of transients performed. For this reason, the first capsule irradiation and examination will be outlined in more detail with discussion of subsequent capsules limited to variations from the general procedure.

IRRADIATION HISTORY

Temperature and reactor power data recorded during TREAT irradiations included the following parameters as a function of time for each of the transients performed:

Instantaneous reactor power
Logarithm of reactor power
Integrated reactor power
Sample fuel temperature (Sample No. 1A only)
Sodium temperature
Inner capsule temperature

The above information was recorded on multichannel high speed photographic recorders (oscillographs), and read by hand or with a Benson-Lehner Chart Reader (OSCAR). In the case of temperatures, readings were taken in millivolts and converted to degrees F using standard tables and applying proper corrections for reference junction temperature.

REACTOR POWER

Table C-1 is a record of significant reactor parameters for all transients performed in Series I. The first three transients on specimen No. 1A were "clipped" by a scram controlled on integrated reactor power. These transients were used as a calibration to predict sample fuel temperature in later tests (see following). TREAT reactor power and the integrated core power as a function of time are illustrated in Figures 19 through 27 for most of the Series I transients (two typical transients only are included for sample No. 1E).

TABLE C-1

TREAT REACTOR PARAMETERS FOR SERIES I TRANSIENTS

Transient APED	No. TREAT	Initial Period Sec.	Reactivity Addition, %K	Integrated Power, MWS	Peak Power MW
1A-1	384	0.369	0.89	19	35
-2	385	0.279	0.98	89	78
-3	386	0.270	1.00	162	88
-4	387	0.140	1.33	315	315
1B-1	404	0.087	1.74	420	832
1C-1	423	0.072	1.97	585	1310
1D-1	438	0.047	2.64	765	3340
1E-1	447	0.060	2.20	383	1770
-2	448	0.065	2.10	573	1560
-3	449	0.063	2.14	480	1545
-4	450	0.063	2.14	580	1500
-5	451	0.063	2.14	576	1525
-6	452	0.063	2.14	580	1520
-7	543	0.065	2.10	575	1490

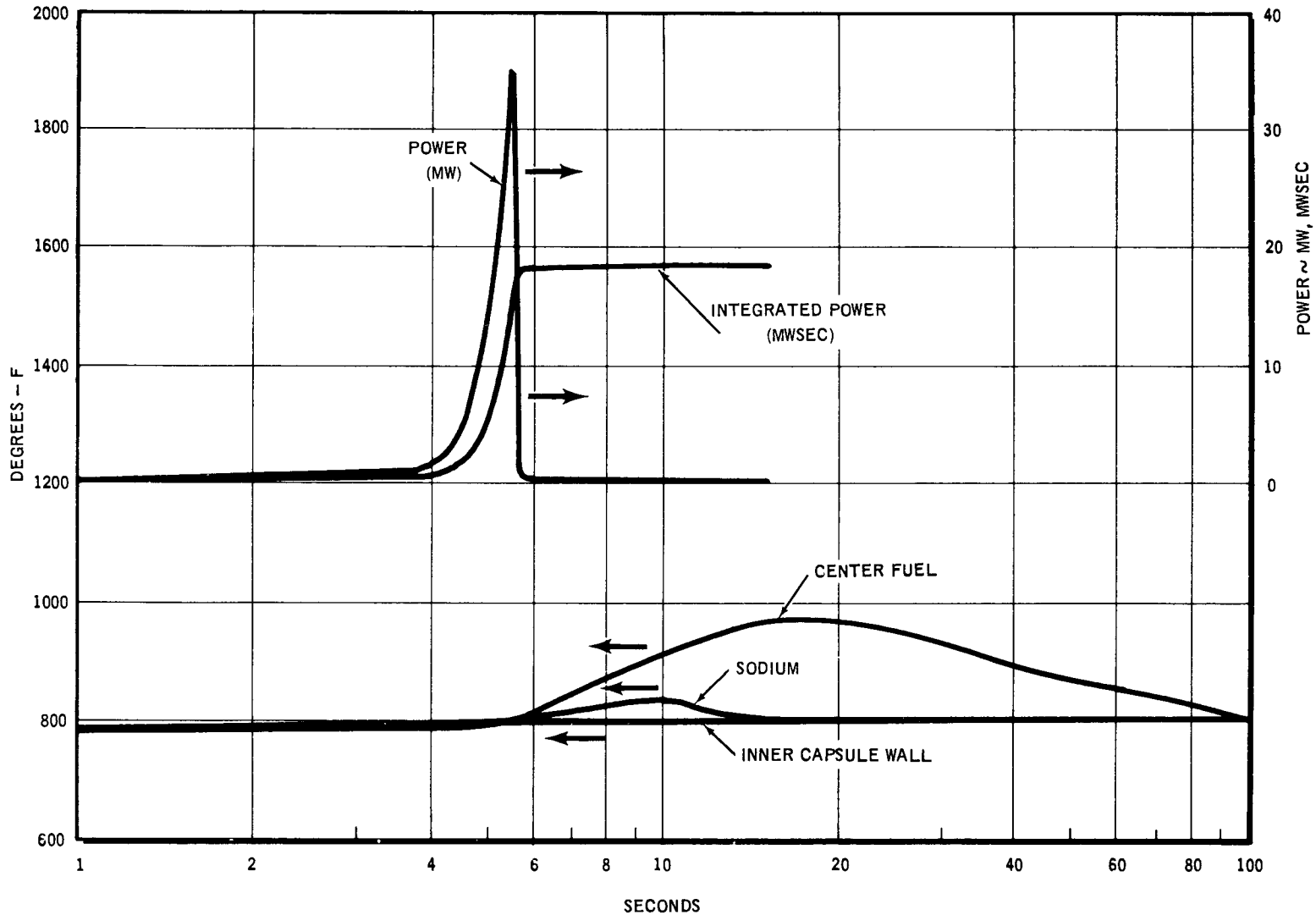

FIGURE 19 TREAT TRANSIENT NO. 384 – APED SAMPLE 1A

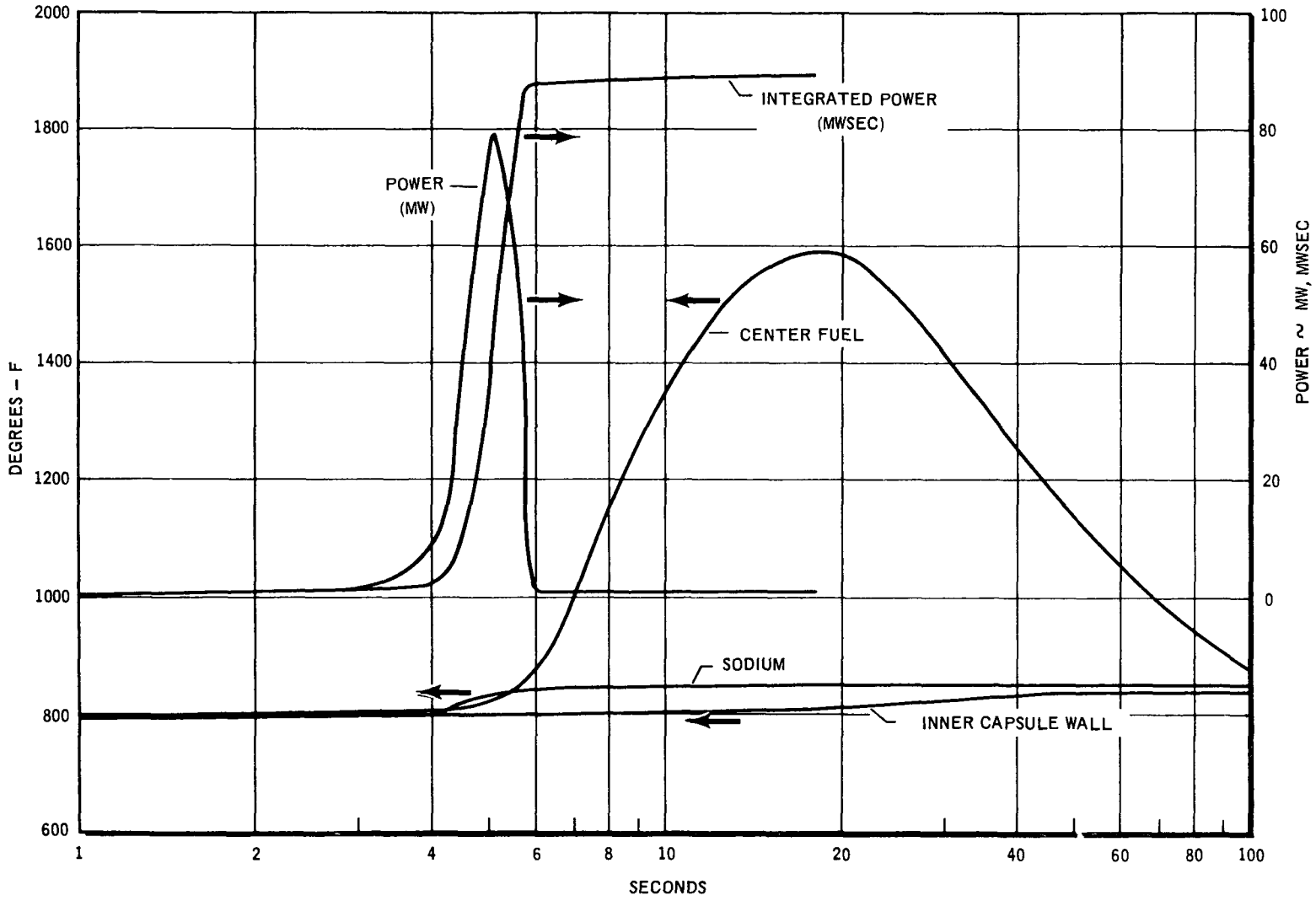

FIGURE 20 TREAT TRANSIENT NO. 385 – APED SAMPLE 1A

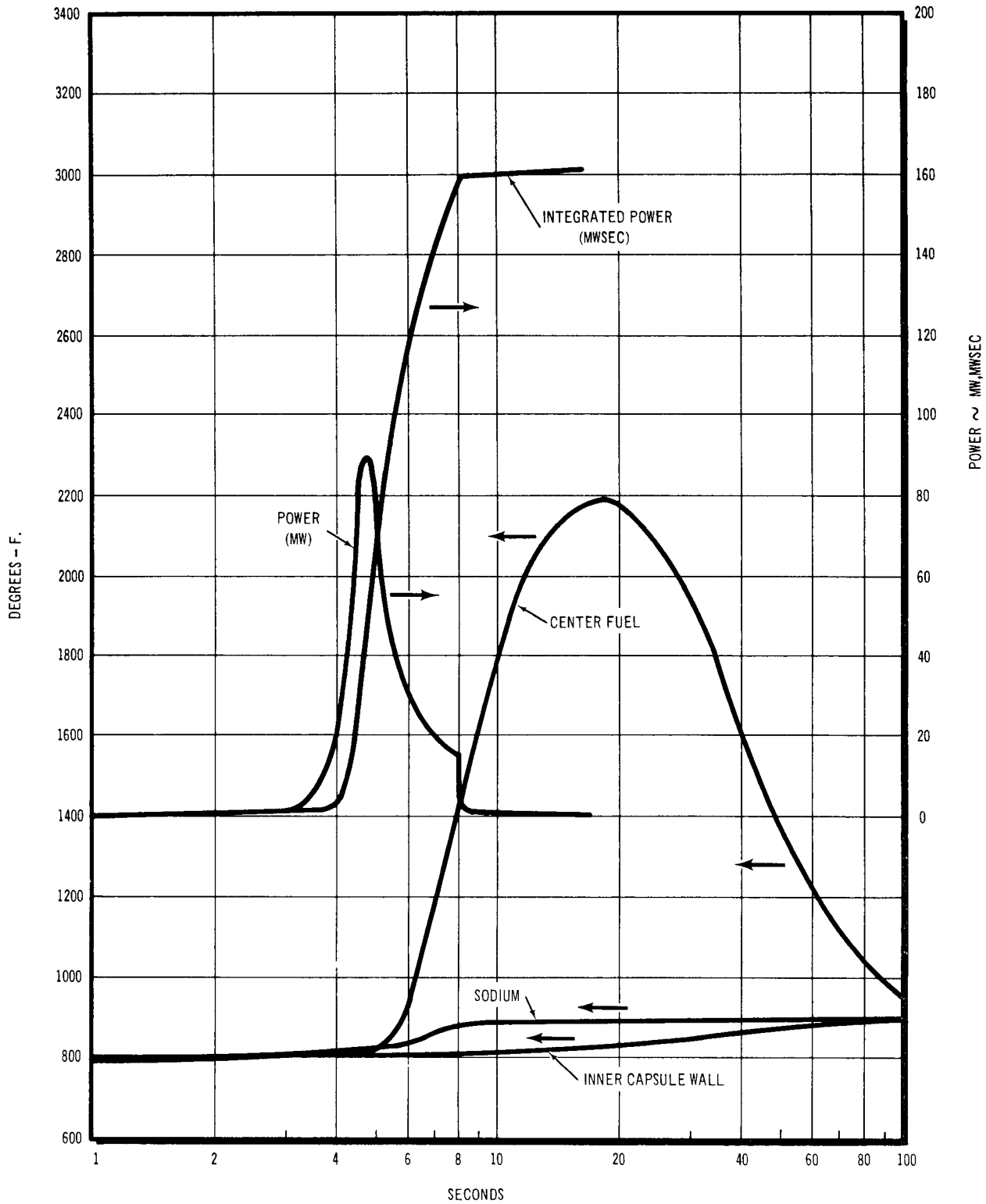

FIGURE 21 TREAT TRANSIENT NO. 386 – APED SAMPLE NO. 1A

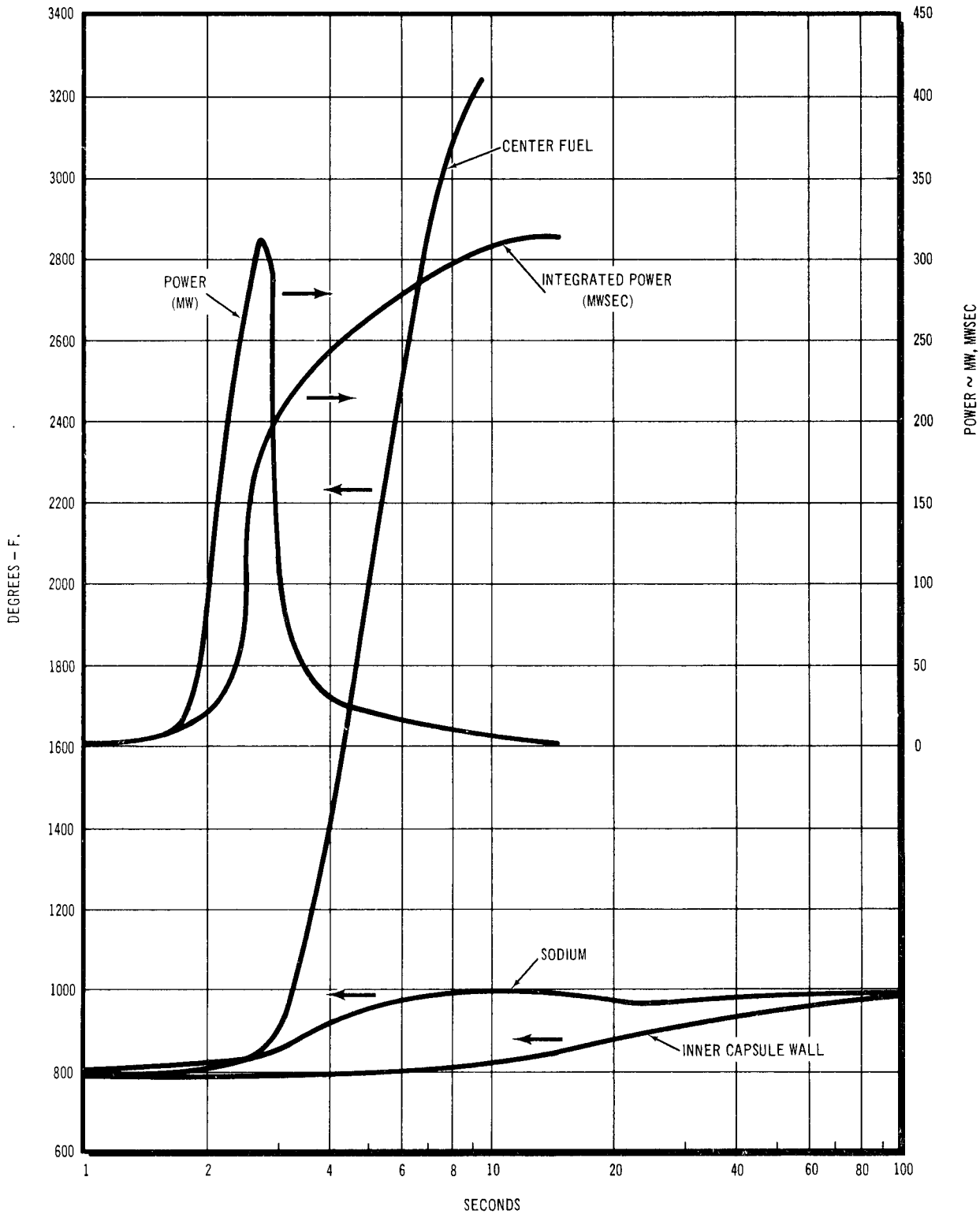

FIGURE 22 TREAT TRANSIENT NO. 387 – APED SAMPLE 1A

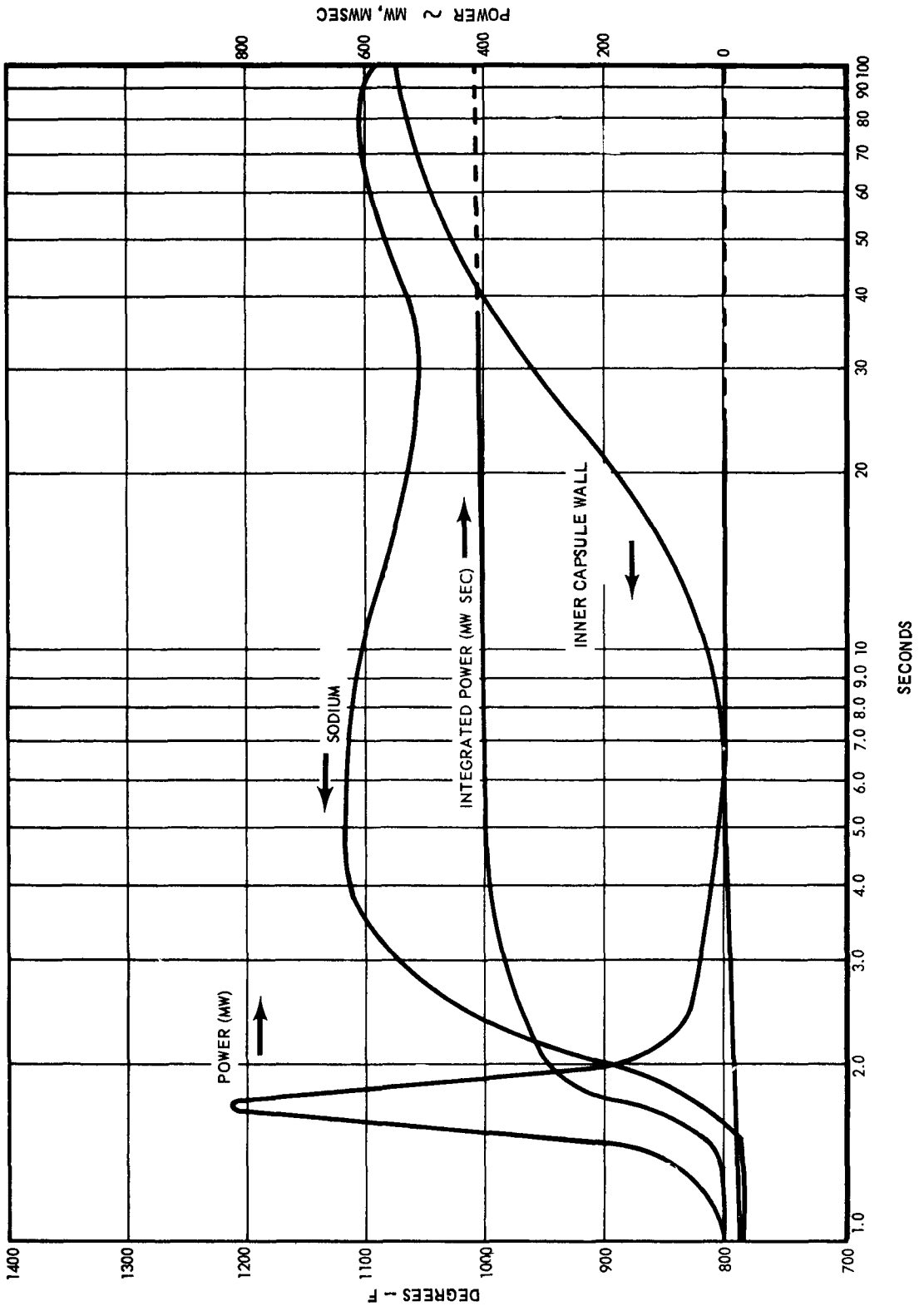

FIGURE 23 TREAT TRANSIENT NO. 404 – APED SAMPLE 1B

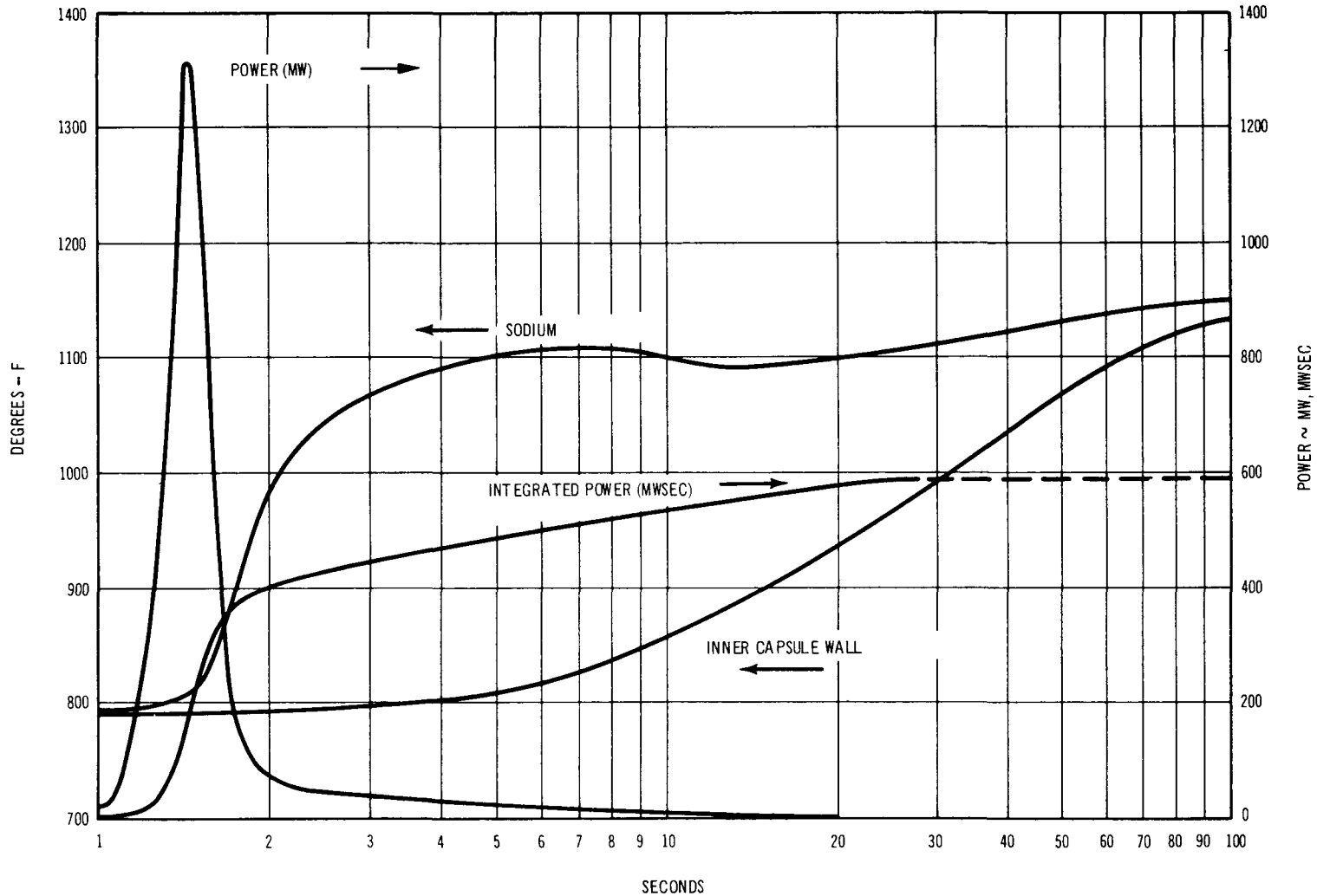

FIGURE 24 TREAT TRANSIENT NO. 423 - APED SAMPLE 1C

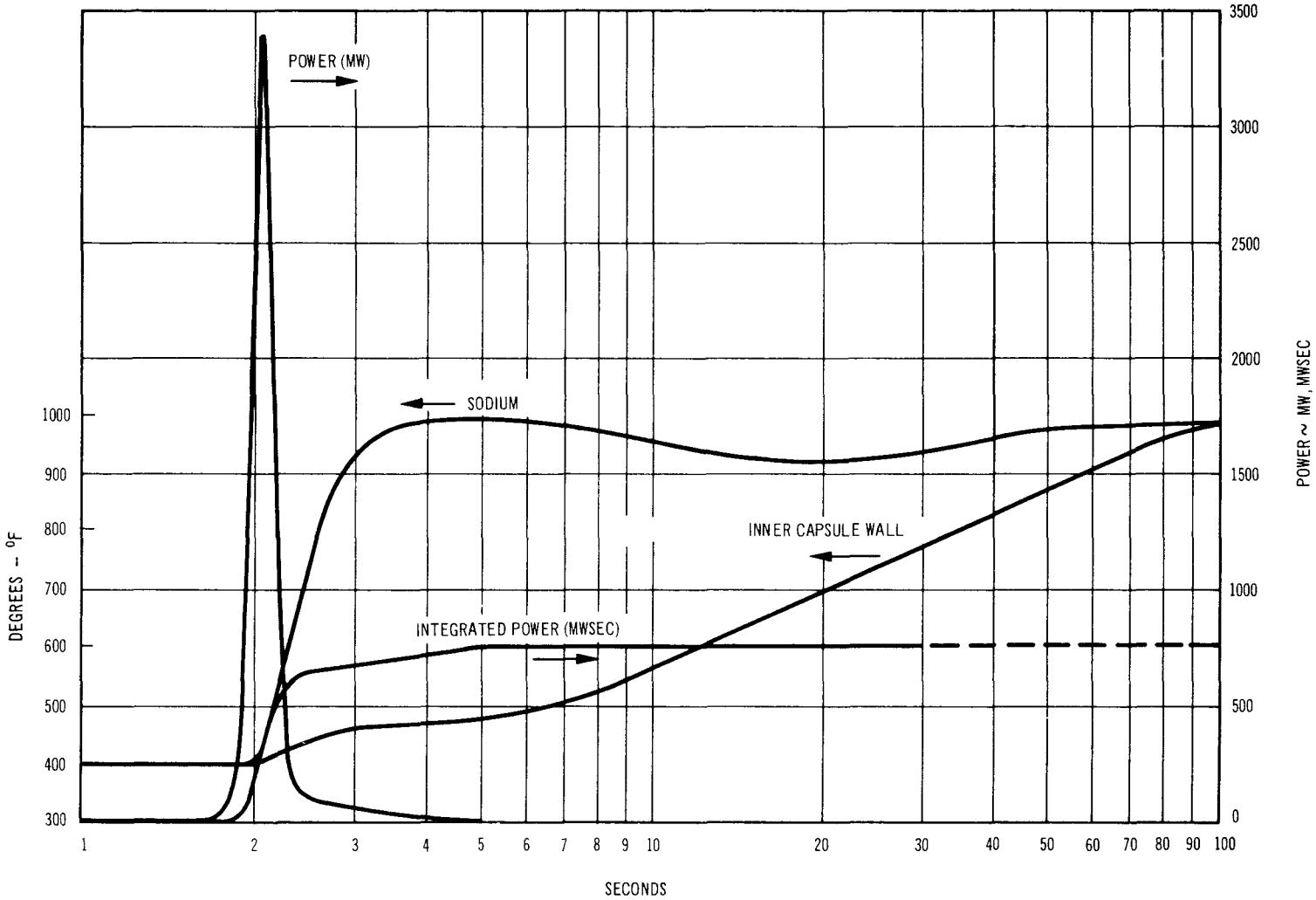

FIGURE 25 TREAT TRANSIENT NO. 438 – APED SAMPLE 1D

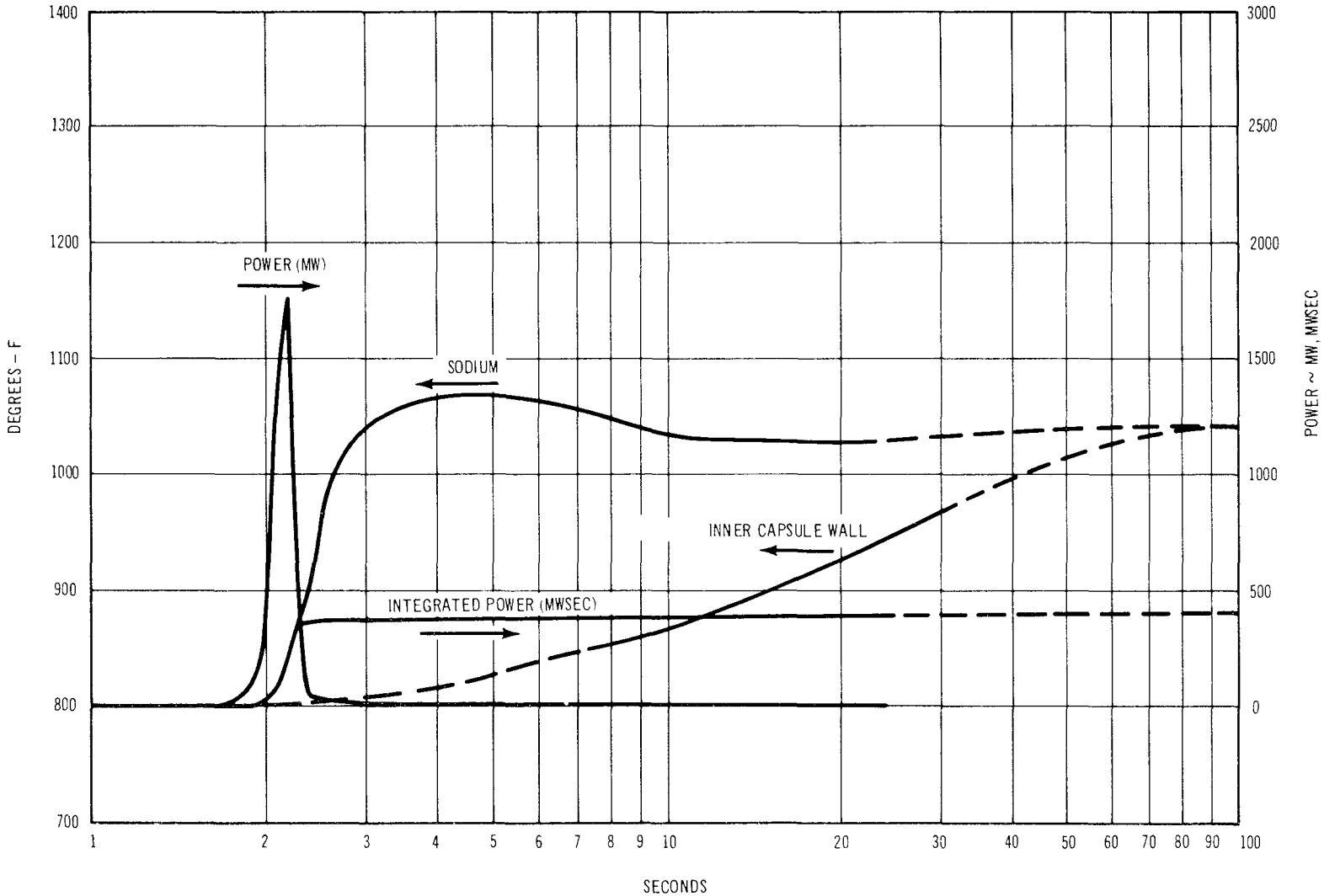

FIGURE 26 TREAT TRANSIENT NO. 447 - APED SAMPLE 1E

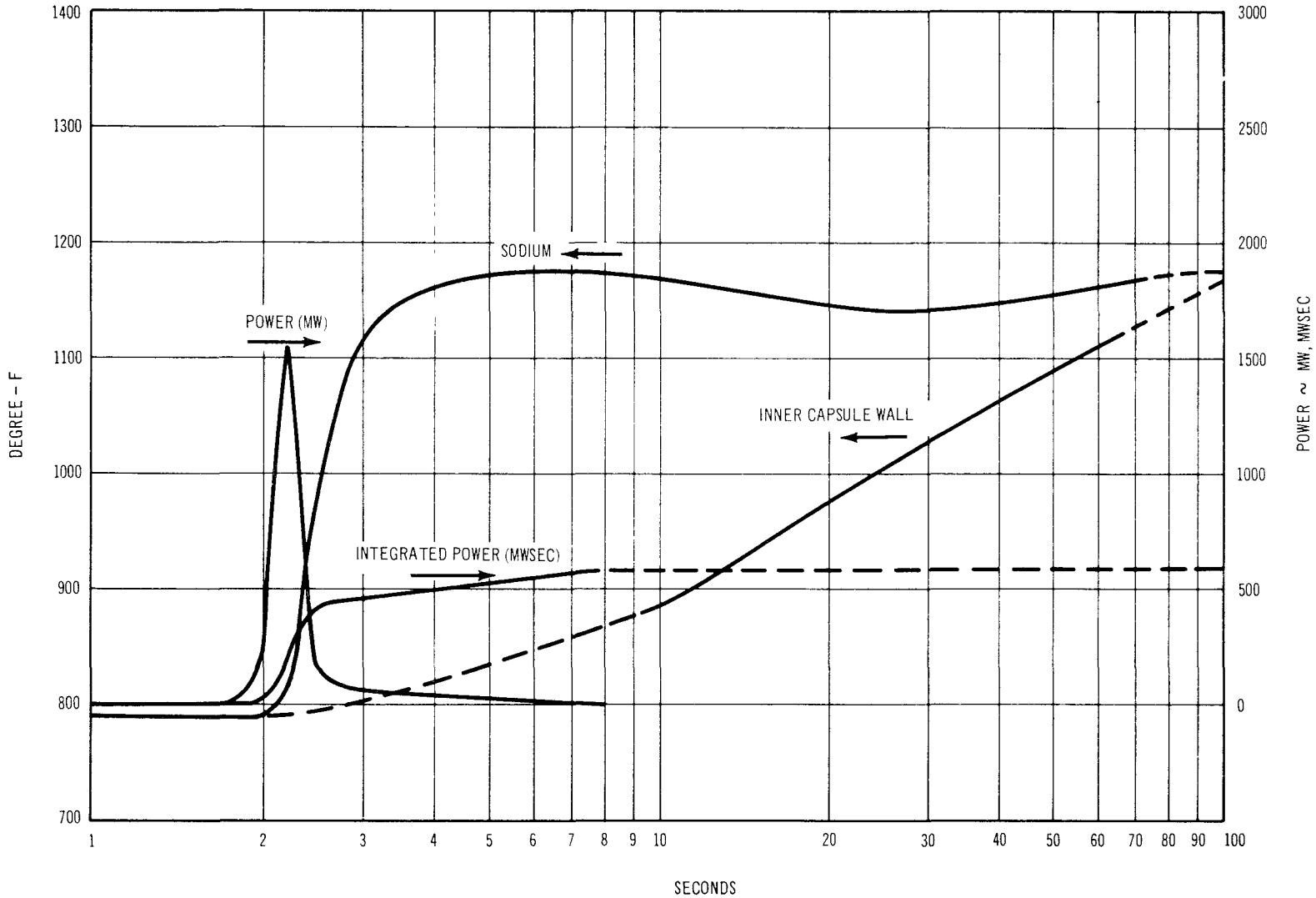

FIGURE 27 TREAT TRANSIENT 448 – APED SAMPLE 1 E

EQUILIBRIUM TEMPERATURE AND SAMPLE POWER

The test capsule was designed to act as a calorimeter and therefore, determination of sample power depends upon accurate measurement of the "equilibrium" temperature of the insulated assembly following a given transient test. In the three preliminary transients on sample No. 1A, it was found that the fuel, sodium, and capsule wall reached essentially the same temperature approximately 100 seconds after the power pulse. Available in-pile cooling curves indicated that the capsule lost only about 4 F/min. when the inner capsule wall was at 800 F. This loss was within the accuracy of the equilibrium temperature determination at 100 seconds.

In order to arrive at the best estimate of equilibrium temperature, the temperature rise at 100 seconds after peak power, of five thermocouples was considered for each transient:

TC's 1 and 2 - sodium temp. (recorded on oscillographs)

TC's 4 and 5 - inner capsule outer wall (oscillographs)

TC and 7 - inner capsule outer wall (heater control couple - Bristol chart recorder)

From an average of these readings, and a capsule heat capacity based on the average capsule temperature during each transient, sample power values were calculated (see Table C-2). Capsule heat capacities were derived from measured heating and cooling rates during pre-irradiation calibration.

TABLE C-2

SERIES I SAMPLE POWERS AND ESTIMATED FUEL TEMPERATURES

Transient No.	Equilibrium Temp. Rise, °F	Total Sample Power, BTU	Estimated Peak Fuel Temp., °F	Est. Max. Volumetric Avg. Fuel Temp., °F
1A-1	12 ± 8	55 ± 38	1090 ± 130	970 ± 120
-2	58 ± 6	268 ± 32	1820 ± 100	1620 ± 100
-3	107 ± 8	496 ± 40	2520 ± 130	2250 ± 120
-4	207 ± 9	973 ± 42	4090 ± 140	3640 ± 130
1B-1	290 ± 11	1366 ± 52	5000 + 0.4 Heat of Fusion	4890 ± 70
1C-1	362 ± 15	1709 ± 70	5290 ± 210	5000 + 0.6 Heat of Fusion
1D-1	567 ± 27	2506 ± 119	7370 ± 400	6570 ± 350
1E-1	244 ± 36	1147 ± 169	4670 ± 570	4160 ± 500
-2	387 ± 38	1827 ± 179	5570 ± 390	5000 + 0.8 Heat of Fusion
-3	392 ± 32	1850 ± 151	5650 ± 300	5000 + 0.9 Heat of Fusion
-4	400 ± 30	1872 ± 140	5710 ± 260	5000 + 0.9 Heat of Fusion
-5	417 ± 29	1960 ± 136	5820 ± 400	5190 (+360-190)
-6	425 ± 16	2023 ± 76	6010 ± 220	5360 ± 200
-7	417 ± 27	1984 ± 129	5920 ± 380	5280 (+340-280)

APPENDIX D

SAMPLE FUEL TEMPERATURES - BASIS FOR ESTIMATES

Table C-2 indicates the estimated sample fuel temperatures for each transient run in Series I. The method used in calculating these temperatures and the assumptions made have been discussed in previous reports, [16] and are summarized only briefly here.

Since the self-shielding effect in our 1 inch dia. specimen results in a large radial temperature gradient, it is necessary to consider three temperatures within the fuel; center fuel temperature, average (volumetric) fuel temperature, and peak fuel temperature. An extrapolation of both time and temperature versus reactor power based on the three preliminary transients on sample No. 1A, indicates that an actual center fuel temperature rise of about 2700 F was realized at some 15 seconds after peak power for the 315 MW second run. This estimate appears reasonable from the fuel TC trace on Figure 22.

If it is assumed that all the heat generated in the sample was effective in raising fuel temperature, a theoretical maximum temperature rise may be calculated. This Delta T applies to the volumetric temperature average of the fuel at its maximum reading. This reading can then be compared to the actual ΔT sensed by the fuel TC on the first three transients on this sample. The ratio of measured fuel temperature rise to the theoretical value above, appeared to be relatively constant at 64 per cent for the three preliminary transients. Applying this ratio to the final transient on sample No. 1A, we can estimate the fuel TC rise at 64 per cent of 4360 F or 2790 F. The probable error assigned to this number is $\pm$ 200 F due to sample power uncertainities. Thus, it is confirmed, by both methods of calculation that on the final transient, the fuel thermocouple attained a temperature between 3500 and 3600 F.

An attempt was made to estimate the volumetric average fuel temperature for the last transient on sample No. 1A, based on sample heat generation and dissipation to the heat sink. It appeared that the net heat contained in the fuel pin (heat generated less heat leakage to assembly) reached a maximum of ~650 Btu at 8 seconds. This amount of heat should have resulted in an average fuel temperature rise of ~3100 F above the 800 F preheat level. Assuming a temperature gradient of ~0.96 center-to-average, the central temperature void would have been some 3750 F. Since this estimate compared favorably with the extrapolated values, it was assumed that the peak temperature was in the range indicated and that the calculation method was valid.

INTEGRATED POWER VS TIME

As previously discussed, the measured fuel temperature rise on the initial transients was only some 64 per cent of the Delta T calculated using the total sample power and the theoretical heat capacity of the fuel over the temperature range involved. This leads to the conclusion that only 64 per cent of the transient sample power insertion was effective in raising the fuel temperature, while the remainder was lost to the surrounding medium; which points up the extremely rapid heat dissapation of the system and its effect upon the fuel temperature in the relatively slow transients available in TREAT (as compared to a fast reactor system). It was recognized that this heat loss from the pin during the fuel temperature rise must decrease with shorter, more severe transients, but the results indicated that over the range of transients involved, this change was apparently small with respect to measurement errors.

A comparison of the power versus time plots for the transients in Series I, indicated that the power insertion for each transient was virtually 100 per cent complete in 15 seconds, with at least 70 per cent of the total integrated power being inserted within a two second interval.

COMPARISON AND DISCUSSION OF RESULTS, TREAT POWER VS SPECIMEN POWER

A comparison of data from all Series I transients provides evidence in support of original assumptions and indicates a relatively consistent pattern of results. The relationship between TREAT reactor power and sample power appeared to be approximately linear over the range of transients run (see Figure 28). Data scatter is believed due to temperature measurement errors and deviation in calibration of TREAT power detectors caused by asymmetry of the reactor loading.

COMPUTER CALCULATIONS USING TIGER V

An effort was made to verify estimated fuel temperature by duplicating measured transient parameters in computer calculations. The TIGER V heat transfer program was again utilized as in the case of pre-irradiation calculations. [1, 8] In order to simulate the temperature versus time relationships for sodium and heat sink temperatures, it was necessary to assume average fuel conductivities in excess of 2.0 BTU/hr-ft F and fuel-clad gap conductance values of 5,000 BTU/hr-ft F or greater. These assumptions resulted in calculated maximum clad Delta T of approximately 1500 F for the extreme transient in sample No. 1D. This corresponds to a peak heat flux in excess of 7×10^6 BTU/hr-ft^2 which appears to be unreasonably high. It was concluded that a more exact simulation of the experimental model was necessary and that the computer program must include

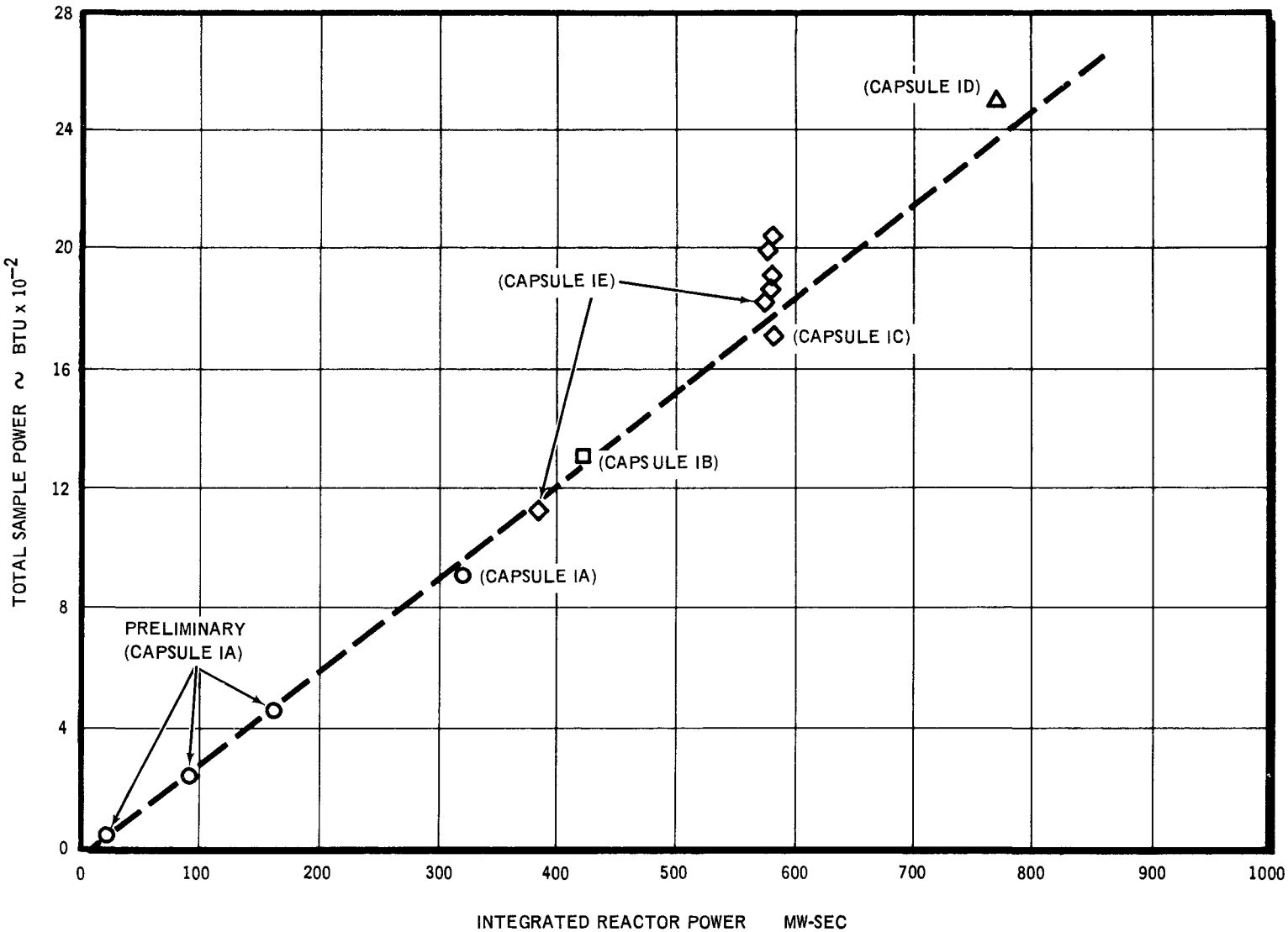

FIGURE 28 SAMPLE POWER VS REACTOR POWER APED – TREAT, SERIES 1

provisions for the variations of material properties with temperature. In the larger transients there is also a need to consider phase changes and heat transfer effects when passing through the heat of fusion of the fuel. For these reasons, a rigorous computer simulation is not feasible at this time and is considered outside the original scope of this qualitative experimental program.

APPENDIX E

POST-IRRADIATION EXAMINATION TECHNIQUES

General

Examination and inspection of the irradiated fuel specimens was similar in each case insofar as method and procedure were concerned. The following paragraphs, therefore, will describe the general techniques employed and cite those instances in which the procedures or results differed substantially from the norm.

Disassembly

Each irradiation assembly was received into the RML, the sodium heated and drained, and the fuel specimen removed prior to transfer to the hot cells for detailed examination. Photographs of a typical irradiation assembly, with the outer shell removed, are shown in Figure 29.

Visual Examinations

Each fuel specimen was visually examined and photographed before and after irradiation. A pattern of discolorations was noted on the exterior surface of all pins following irradiation. This pattern was presumed due to heat as it correponded to the location of pellets within the tube and became more pronounced with increased transient size (and therefore Na temperatures). An apparent crack was noted in the area of one of the spot welds on sample No. 1A, but it was later shown via metallographic examination that there was no significant cladding penetration.

In most areas the post-irradiation exterior appearance of all pins was similar with the exception of sample No. 1E. In this case the cladding surface revealed a considerable amount of deformation. At some points the cladding had expanded, while at other locations severe indentations and warping was noted.

Gamma Scanning

Due to the low burnup in the fuel, it was not possible to gamma scan the capsule using the fission product activity in the fuel. Therefore, an alternate technique, using transmitted activity, was used in order to determine the physical dimensions and location of the fuel and other components within the specimens.

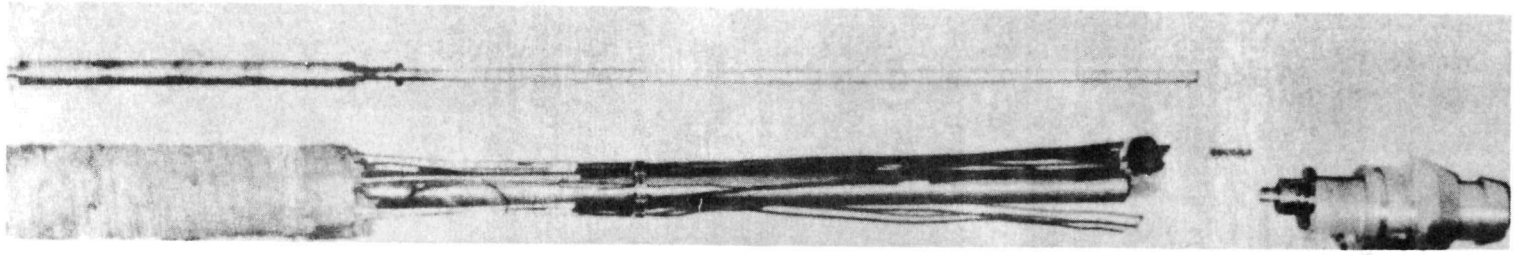

PRE-IRRADIATION

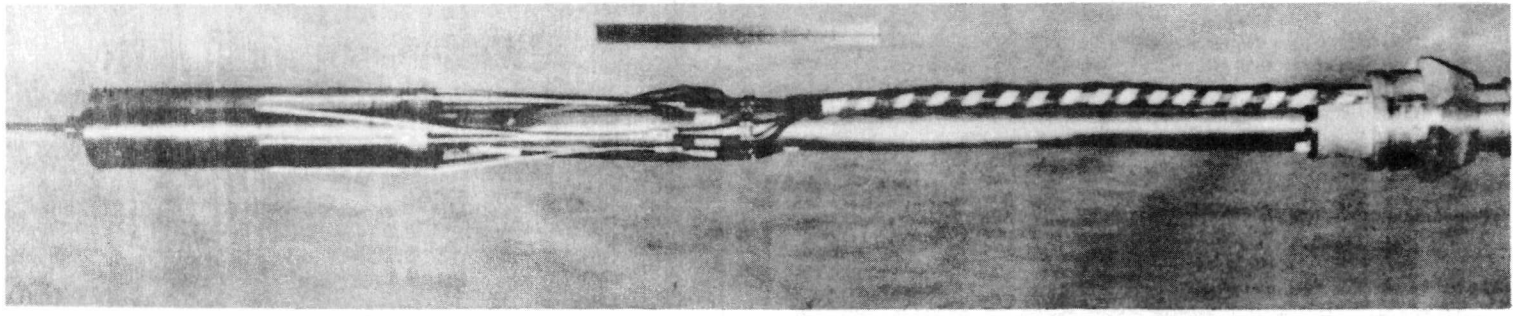

POST-IRRADIATION

FIGURE 29 CAPSULE 1A INTERNAL COMPONENTS OF IRRADIATION ASSEMBLY

A reproduction of a typical set of gamma scans is shown on Figure 30 along with notes relating to the scan and the internal components. Using this technique, it was possible to distinguish the pellet interfaces and, by measuring the length of a stack of pellets on the strip chart recording, it was possible to determine the length of the pellet stacks. Use of this technique with a known length standard showed that such measurements are accurate to ± 0.008 inch.

Dimensional Measurements

Post-irradiation measurements of each fuel pin were taken and compared with pre-irradiation data. Diametral measurements were made using a surface plate and dial gage arrangement capable of readings to the nearest 1/2 mil. Length measurements were made by comparison against a known 14 inch standard prepared specifically for this purpose. Angular orientation was recorded from a scribe mark fabricated on the lower end plug of each sample.

Burnup Analysis

A representative sample of the fuel was taken from each specimen and radiochemically analyzed to determine the burnup. Results of these analyses are summarized in Table VI-1 and were found generally to show good correlation to the integrated reactor power numbers supplied by TREAT.

Sectioning and Visual Inspection

Each fuel pin was sectioned into several lengths by transverse cuts at selected locations. Some of these lengths were then slit longitudinally to expose the pellet surfaces while others were prepared for metallographic examination. Figure 31 is an example of a sectioning diagram showing a typical pattern for sample preparation. The metallographic sections were filled with a Hysol resin compound to hold the fuel in place during subsequent grinding and polishing operations.

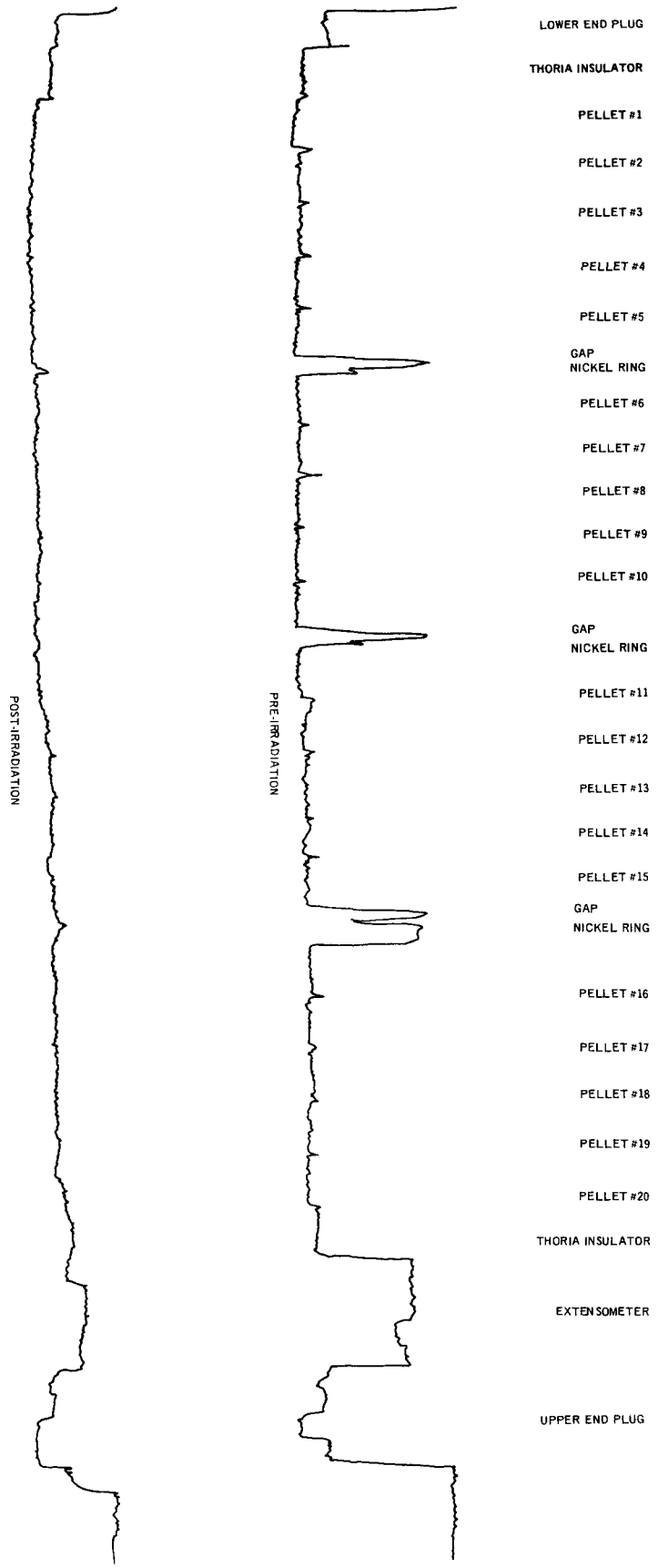

FIGURE 30 PRE AND POST IRRADIATION GAMMA SCANS OF SAMPLE 1D

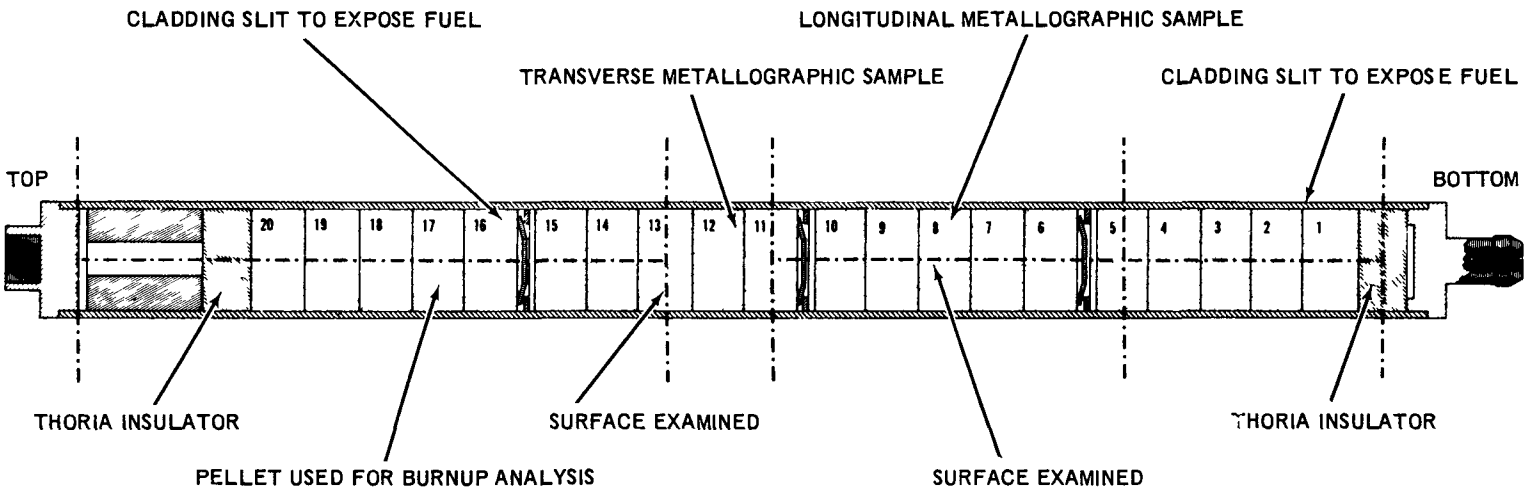

FIGURE 31 CAPSULE 1B, SECTIONING DIAGRAM AND SAMPLE LOCATIONS

BIBLIOGRAPHY

1. Osborn, Sherer, Analytical Studies of Transient Effects in Fast Reactor Fuels; GEAP-4058, August, 1962.

2. Lyons, et al. Central Melting In UO_2 Pellet Fuel-Capsule Irradiation; GEAP-3942 (to be published).

3. Horst, Hutchins, Leitz, Wolfe, Core Design Study for a 500 MWe Fast Oxide Reactor; GEAP-3721-AEC, December, 1961.

4. Cohen, McNelly, Wolfe, Experimental Fast Oxide Reactor; GEAP-3856, November, 1961.

5. Greebler, Hutchins, Sueoka, Calculation of Doppler Coefficient and Other Safety Parameters for a Large Fast Oxide Reactor; GEAP-3646

6. Freund, Elias, MacFarlane, Geier, Boland, Design Summary Report on the Transient Reactor Test Facility - TREAT; ANL-6034, June, 1960.

7. Kirn, Boland, Lawroski, Cook, Reactor Physics Measurements in TREAT; ANL-6173, October, 1960.

8. Fast Ceramic Reactor Development Program; First Quarterly Report, October-December, 1961, GEAP-3888.

9. Fast Ceramic Reactor Development Program; Third Quarterly Report, April-June, 1962, GEAP-3981.

10. Horst, Experimental Fast Ceramic Reactor Design - Status Report as of October 31, 1961; GEAP-3885, April, 1962.

11. Mangrum, Megerth, Pre-Irradiation Data on N. S. Savannah Core II -4, -5, and -6 Prototype Fuel Assemblies to be Tested in VBWR; GEAP-3376 (Addendum), September 1, 1960.

12. Burdick, Parker, Effect of Particle Size on Bulk Density and Strength Properties of Uranium Dioxide Specimens; Journal of the American Ceramic Society, Vol. 39, No. 5, May 1, 1956.

13. MacEwan, Grain Growth in Sintered Uranium Dioxide; AECL-1184, 196.

14. Fast Ceramic Reactor Development Program; Fourth Quarterly Report, July-Sept., 1962, GEAP-4080.

15. Hazards Analysis and Test Specifications for Proposed APED Program in TREAT; approved by K. P. Cohen, October 18, 1962.

16. Fast Ceramic Reactor Development Program; Second Quarterly Report, January-March, 1962, GEAP-3957.